

JPL Publication 02-07



2001 Annual Report – Climate Variability Program

*David Halpern, Editor
Jet Propulsion Laboratory, Pasadena, California*

**National Aeronautics and
Space Administration**

**Jet Propulsion Laboratory
California Institute of Technology
Pasadena, California**

April 2002

The research described in this publication was carried out, in part, at the Jet Propulsion Laboratory, California Institute of Technology, under a contract with the National Aeronautics and Space Administration. Reference herein to any specific commercial product, process, or service by trade name, trademark, manufacturer, or otherwise, does not constitute or imply its endorsement by the United States Government or the Jet Propulsion Laboratory, California Institute of Technology.

Abstract

The Annual Report of the Climate Variability Program briefly describes research activities of Principal Investigators who are funded by NASA's Earth Science Enterprise Research Division. The report is focused on the year 2001. Utilization of satellite observations is a singularity of research on climate science and technology at JPL. Research at JPL has two foci: generate new knowledge and develop new technology.

Acknowledgements

I especially thank the Principal Investigators for their tremendous support. I am grateful to Edward Sewall, who assembled the report, and to Dr. Steven Bard, Manager of Earth Science and Advanced Concepts Office, who provided financial support.

Contents

Page

Abstract	iii
Acknowledgements	iv
Introduction	1
Table 1. NASA Earth Science Enterprise Strategic Plan questions about how the Earth is changing and what the consequences for life on Earth are, and Principal Investigator's name with a 1-page research statement associated with a specific question.....	2
Research Statements	5
Interannual Variability of Snow and Ice and the Carbon Cycle (M. Allen)	7
Phytopia: Discovery of the Marine Ecosystem (C. H. Atkinson)	8
Quantifying the Information Content in the GPS Slant Path Delays (Y. Bar-Sever)	9
The Primary Production Algorithm Round-Robin 3 (PPARR3) (M.-E. Carr)	10
Ice Sheet Basal Processes and Ice Paleoclimate Information (F. Carsey)	11
Pacific Climate Variability and Its Impact on the Central California Coastal Upwelling (Y. Chao)	12
Interannual and Decadal Fluctuations in Atmospheric Angular Momentum (AAM) and Sea Surface Temperature (SST): Links among the Earth's Subsystems (J. O. Dickey)	13
Comparison of ARMAR and TRMM PR Measurements (S. L. Durden).....	14
Intraseasonal Sea Level Variability from Altimeter Sea Level and Scatterometer Winds (L.-L. Fu)	15
Satellite Data Assimilation (I. Fukumori)	16
Large-Scale Oceanic Wave Processes (R. E. Glazman)	17
Oceanic Angular Momentum and the Earth's Rotation (R. Gross)	18
Using Global Terrestrial GPS Measurements to Unravel the Emerging Altimetric Record of Global Sea-Level Change (B. Haines)	19

Contents (Continued)

	<u>Page</u>
Research Statements (Continued)	
GPS Radio Occultations Coming of Age: Two Spacecraft Launches Add Two New Instruments for Climate Monitoring (G. Hajj)	20
Sensitivity of Computed Equatorial Ocean Currents to Wind and Data Assimilation (D. Halpern).....	21
Water Vapor in the Lower Stratosphere and Upper Troposphere (R. Herman).....	22
Small Scale Coastal Eddies and Hazards off California (B. Holt).....	23
Rainfall Observations Using an Airborne Dual-Frequency Radar (E. Im)	24
Postglacial Rebound and Ice Mass Change in Antarctica and Patagonia (E. R. Ivins).....	25
Positive Mass Balance of the Ross Ice Streams, West Antarctica (I. Joughin)	26
Seasonal Sea Ice Deformation, Growth, and Production (R. Kwok).....	27
Hurricane Studies with the High Altitude MMIC Sounding Radiometer (HAMSR) (B. H. Lambriksen).....	28
Interannual to Decadal Variation in Tropical-Subtropical Exchange Processes (T. Lee).....	29
Sea Surface Salinity Remote Sensing (F. K. Li)	30
Ocean-Atmospheric Interaction in Climate Change (W. T. Liu)	31
Microwave Temperature Profiler (MTP) for CAMEX-4 (M. J. Mahoney).....	32
Geodetic Signatures of Intraseasonal–Interannual Changes in the Climate System (S. L. Marcus).....	33
Sea Ice and Global Ocean Circulation (D. Menemenlis)	34
Integrated Instrumentation for the JPL Cryobot: The Dust Sensor (C. T. Mogensen)	35
Timing and Scales of Arctic Sea Ice Albedo Transitions Observed with RADARSAT-1 Data and RGPS Products (S. V. Nghiem)	36
Corals Impacted by Interannual and Decadal Climate Variability (W. C. Patzert)	37

Contents (Continued)

Page

Research Statements (Continued)

Importance of the Indonesian Throughflow (ITF) to Understand and Predict El Niño/La Niña Events in the Pacific (C. Perigaud).....	38
Ionospheric Calibration for Ocean Altimeters (X. Pi)	39
The Impact of Volcanic Emissions on the Regional Environment (V. J. Realmuto)	40
Satellite Radar Observations of the Mass Balance of Polar Ice Sheets (E. Rignot).....	41
Study of Coastal Ocean Dynamics for Predicting Coastal Environmental Changes (Y. T. Song).....	42
Synergistic Use of TRMM and SeaWinds Data (M. W. Spencer).....	43
Vertical Distribution of Aerosol Backscatter over the Pacific Ocean (D. Tratt)	44
2-cm GPS Altimetry over Crater Lake (R. Treuhaft).....	45
CloudSat Mission Observations Will Improve Understanding of Cloud-Climate Interactions (D. Vane)	46
Polarimetric Radar Remote Sensing of Ocean Wind (S. H. Yueh).....	47
Effect of Wind Stress Parameterization on an Ocean Model and GRACE Ocean Validation (V. Zlotnicki).....	48
GPS Altimetry (C. Zuffada)	49
Appendix A. 2000–2001 Publications	51
Appendix B. Acronyms	63



Introduction

The 2001 Annual Report of the Climate Variability Program briefly describes activities funded by NASA's Earth Science Enterprise Research Division, known as NASA Code YS. The JPL Climate Variability Program is the 8312 component of the JPL Earth Science and Technology Directorate. The JPL Climate Variability Program encompasses physical and biological attributes of Earth's climate.

Utilization of satellite observations is a singularity of research on climate science and technology at JPL. Research at JPL has two foci: generate new knowledge and develop new technology.

The report is focused on the year 2001. Because seeds of research may not blossom in a year, the list of peer-referenced publications includes those for 2000 and 2001. In addition, the Principal Investigator's 1-page research statement is an opportunity to extend the coverage of research into 2002. For many Principal Investigators, the 1-page research statement does not adequately describe the breadth of their research activities. Many Principal Investigators had to choose a research topic among multiple topics.

The NASA Earth Science Enterprise Strategic Plan (available at <http://www.earth.nasa.gov>) has three goals: (1) observe, understand, and model the Earth system to learn how it is changing, and the consequences for life on Earth; (2) expand and accelerate the realization of economic and societal benefits from Earth science, information, and technology; and (3) develop and adopt advanced technologies to enable mission success and serve national priorities. Goal 1 addresses 23 scientific questions, and the alignment of the questions and the Principal Investigator 1-page research statements is described in Table 1.

Further information may be obtained from the Principal Investigator, whose coordinates are provided on the 1-page research statement, or by contacting Dr. David Halpern, Manager, Climate Variability Program, MS 300-323, Jet Propulsion Laboratory, 4800 Oak Grove Drive, Pasadena, CA 91109-8099 (tel, 818-354-5327; fax, 818-393-1734; email, david.halpern@jpl.nasa.gov).

Table 1. NASA Earth Science Enterprise Strategic Plan questions about how the Earth is changing and what the consequences for life on Earth are and Principal Investigator's name with a 1-page research statement associated with a specific question.

How is the global Earth system changing? (Variability)

How are global precipitation, evaporation, and the cycling of water changing?

Bar-Sever, Yoaz
Durden, Stephen L.
Herman, Robert
Im, Eastwood

How is the global ocean circulation varying on interannual, decadal, and longer time scales?

Dickey, Jean O.
Fu, Lee-Lueng
Fukumori, Ichiro
Glazman, Roman E.
Halpern, David
Lee, Tong
Li, Fuk K.
Menemenlis, Dimitris
Pi, Xiaoqing
Yueh, Simon H.
Zlotnicki, Victor
Zuffada, Cinzia

How are global ecosystems changing?

Atkinson, Cynthia Hall

How is stratospheric ozone changing, as the abundance of ozone-destroying chemicals decrease and new substitutes increase?

What changes are occurring in the mass of the Earth's ice cover?

Carsey, Frank
Joughin, Ian
Kwok, Ron
Nghiem, Son V.
Rignot, Eric

What are the motions of the Earth and the Earth's interior, and what information can be inferred about Earth's internal processes?

Gross, Richard
Ivins, Erik R.
Mogensen, Claus Tilsted

What are the primary forcings of the Earth system? (Forcing)

What trends in atmospheric constituents and solar radiation are driving global climate?

Tratt, David M.

What changes are occurring in global land cover and land use, and what are their causes?

How is the Earth's surface being transformed and how can such information be used to predict future changes?

How does the Earth system respond to natural and human-induced changes?

(Response)

What are the effects of clouds and surface hydrologic processes on Earth's climate?

Vane, Deborah

How do ecosystems respond to and affect global environmental change and the carbon cycle?

Allen, Mark

Carr, Mary-Elena

Holt, Benjamin

How can climate variations induce change in the global ocean circulation?

How do stratospheric trace constituents respond to change in climate and atmospheric composition?

How is global sea level affected by climate change?

What are the effects of regional pollution on the global atmosphere, and the effects of global chemical and climate changes on regional air quality?

Realmuto, Vincent J.

What are the consequences of change in the Earth system for human civilization?

(Consequences)

How are variations in local weather, precipitation, and water resources related to global climate variation?

What are the consequences of land cover and land use change for the sustainability of ecosystems and economic productivity?

What are the consequences of climate and sea level changes and increased human activities on coastal regions?

Chao, Yi

Patzert, William C.

Song, Y. Tony

Treuhaf, Robert

How well can we predict future changes to the Earth system? (Prediction)

How can weather forecast duration and reliability be improved by new space-based observations, data assimilation, and modeling?

Lambrigtsen, Bjorn H.

Mahoney, Michael J.

Spencer, Michael W.

How well can transient climate variations be understood and predicted?

Liu, W. Timothy

Marcus, Steven L.

Perigaud, Claire

How well can long-term climatic trends be assessed or predicted?

Haines, Bruce

Hajj, George

How well can future atmospheric chemical impacts on ozone and climate be predicted?

How well can cycling of carbon through the Earth system be modeled and how reliable are predictions of future atmospheric concentrations of carbon dioxide and methane?

Research Statements



Interannual Variability of Snow and Ice and the Carbon Cycle

Mark Allen

tel, 818-354-3665; fax, 818-393-4445; email, mark.allen@jpl.nasa.gov

NASA Earth Science Enterprise Strategic Plan Question

How do ecosystems respond to and affect global environmental change and the carbon cycle?

The goal of this research is to understand the impact of the interannual variability in snow/ice on the carbon cycle. The effect of snow/ice on the biosphere, especially on the CO₂ production and removal rates, will be studied using global satellite data sets acquired in the last two decades and a biospheric model to simulate the CO₂ interannual variability at high latitudes.

In the last year we have concentrated on identifying the global patterns of change in the hydrological cycle and generalizing the Caltech/JPL 2-D model to 3-D, so that the spatial and temporal patterns of CO₂ can be modeled. This will be briefly described as follows.

Using the TOMS (Total Ozone Mapping Spectrometer on Nimbus 7) data, we obtained the interannual variability for the Earth's UV albedo derived from TOMS reflectivity, as shown in Fig. 1. While the average albedo variability is very small for most of the planet, on the order of 1%, there is a large variability on land resulting from variability in snow/ice coverage. These land albedo changes cannot be explained by cloud variability, as is clear from the lack of variability over the ocean at similar latitudes

The Caltech/JPL 2-D model for modeling the photochemistry and transport of trace species is being generalized to 3-D; winds will be derived from the GISS GCM model. The mechanics of the 3-D model recently have been implemented and tested. The current plan is to apply this model to study the interannual variability of atmospheric carbon dioxide and compare with observations. It is expected that snow/ice has a major effect in modulating the growth season, and thus the net sink of CO₂.

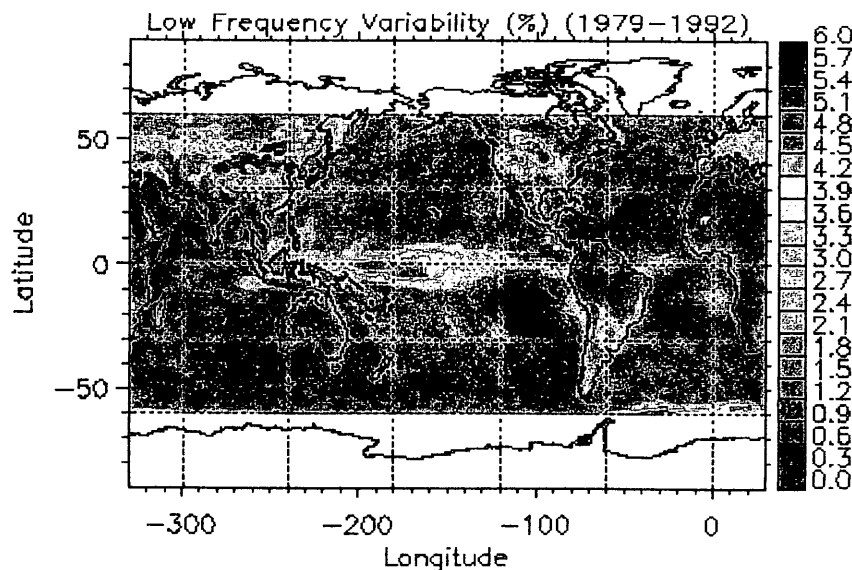


Figure 1. The interannual variability for the Earth's UV albedo derived from TOMS reflectivity. The interannual variability is computed using the standard deviation of the interannual anomaly data, which is the residue after the seasonal cycle is removed. Data taken from TOMS Version 7, 1979-1992.

Phytopia: Discovery of the Marine Ecosystem

Cynthia Hall Atkinson

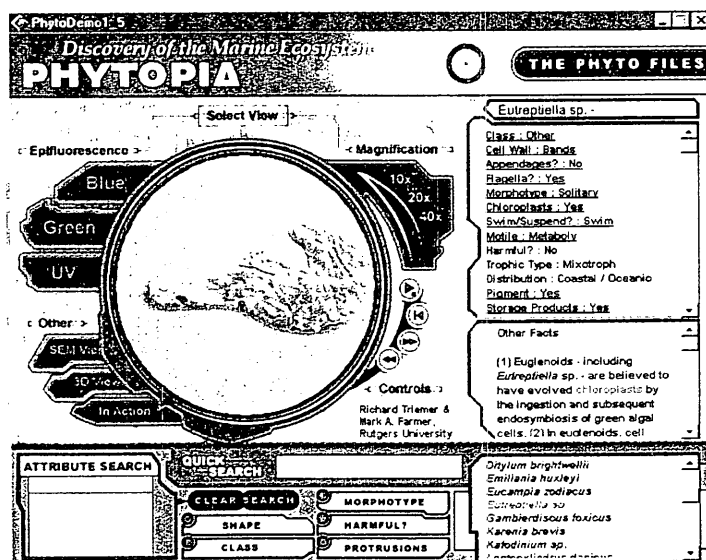
tel, 818-354-9017; fax, 818-393-3405; email, Cynthia.H.Atkinson@jpl.nasa.gov

NASA Earth Science Enterprise Strategic Plan Question

How are global ecosystems changing?

Phytopia is an educational CD-ROM now being developed by the Bigelow Laboratory for Ocean Sciences (Bigelow Laboratory), the University of New England, and the Data Distribution Laboratory at the Jet Propulsion Laboratory. This multimedia educational experience brings the lower end of the marine food web "to life," promoting interaction with multimedia tools that enable students to discover why the marine ecosystem is critical to human existence.

The core technology of Phytopia is a searchable database of many important phytoplankton from the world's temperate oceans: "The Phyto Files." This module contains 36 species of important temperate marine phytoplankton species. Each phytoplankton species has numerous attributes that outline its unique form and function, such as cell wall type, morphotype, motility, harmfulness, shape, etc. Multimedia tools allow the user to search through the phytoplankton list by scrolling through the list, by typing in the name of the phytoplankton, or by specifying certain attributes—shape, class, morphotype, harmfulness, and protrusion type (i.e., appendages or flagella). The database is completely scalable and the programming contains little "hard-coding" to allow for future expansion in order to include rarer temperate forms as well as polar and tropical species. Also included in "The Phyto Files" module are three-dimensional phytoplankton models that can be manipulated in space and viewed from any perspective. A virtual microscope tool allows the user to view prepared assemblages of phytoplankton at different magnifications, under different epifluorescence conditions, or by scanning electron microscopy. This tool gives the user the "look and feel" of modifying the excitation bands and magnification of a microscope. The 36 species represented in the database can be displayed at pre-determined magnification settings. Certain species can be viewed by scanning electron microscopy techniques, enhancing one's ability to distinguish the structure and form of the phytoplankton. For some species, the user can view movies showing the motility, reproduction, and morphology.



Quantifying the Information Content in the GPS Slant Path Delays

Yoaz Bar-Sever

tel, 818-354-2665; fax, 818-393-6890; email, yoaz.bar-sever@jpl.nasa.gov

NASA Earth Science Enterprise Strategic Plan Question

How are global precipitation, evaporation, and the cycling of water changing?

We quantify, for the first time, the amount of information on atmospheric water vapor that can be extracted from the Global Positioning System (GPS) line-of-sight measurement, utilizing a collocated GPS receiver and a pointed water vapor radiometer (WVR) at the Cloud and Radiation Testbed site near Lamont, Oklahoma. The data used in this study were collected over a 30-day period in July and August 1999, during which the GPS receiver was able to track up to 12 satellites simultaneously. The WVR was programmed to follow a schedule where it measured the atmospheric emission in the direction of the GPS satellites. We processed the GPS data using the GIPSY-OASIS II software package, solving for a zenith tropospheric delay and horizontal delay gradients. The line-of-sight measurements were constructed by combining the zenith delay estimates, delay gradient estimates, and the post-fit residuals.

By applying the same estimation technique to the GPS and the WVR data, we were able to demonstrate that the GPS-based gradients match the WVR-based gradients remarkably well (see figure). The gradients capture the first-order variability in the horizontal distribution of water vapor in the troposphere; recall that the zero order approximation assumes horizontal symmetry and is quantified by the zenith delay. We found that the higher-order information (second order variability and higher) is not captured well with signal-to noise problems. We conclude that most observations of slant path delays to date are merely representations of the delay gradients, and has major implications for atmospheric tomography.

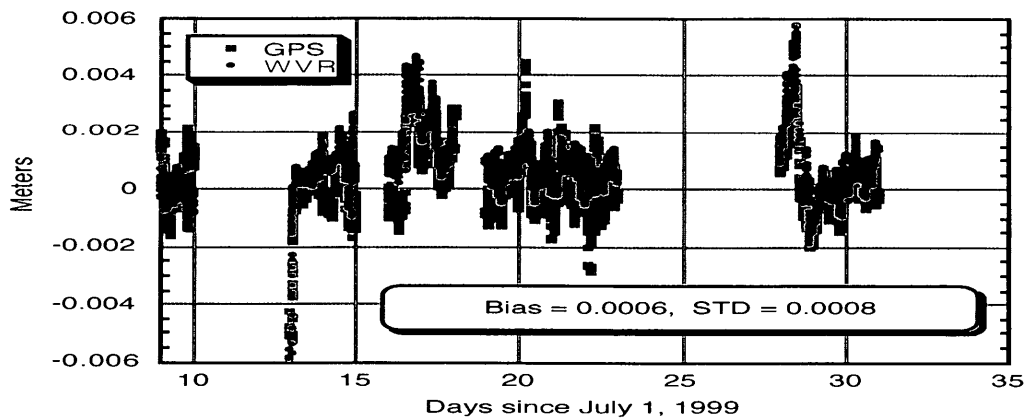


Fig. 1. The north component of the tropospheric delay gradient as estimated from GPS data and WVR data. The gradient was estimated from each data type using a Kalman filter followed by a backward smoother.

The Primary Production Algorithm Round-Robin 3 (PPARR3)

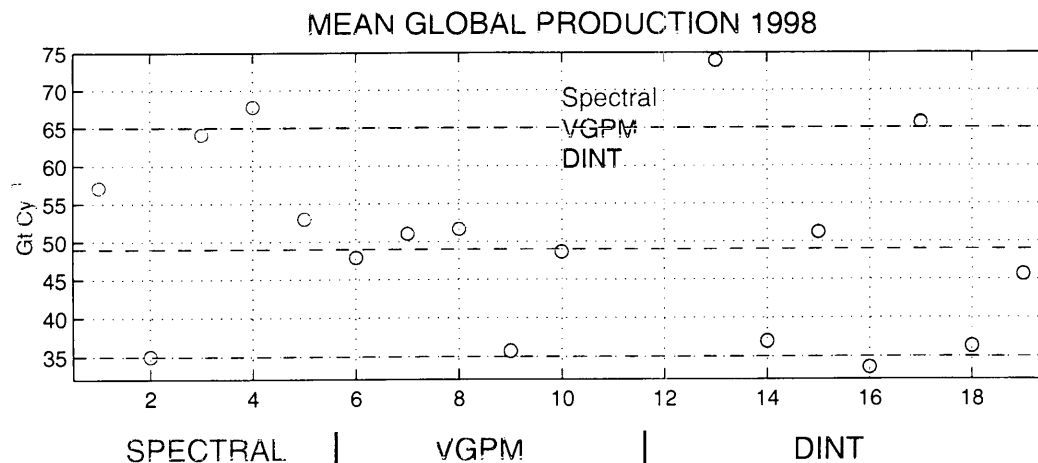
Mary-Elena Carr

tel, 818-354-5097; fax, 818-393-6720; email, mec@pacific.jpl.nasa.gov

NASA Earth Science Enterprise Strategic Plan Question:

How do ecosystems respond to and affect global environmental change and the carbon cycle?

Photosynthetically fixed carbon, or primary production, plays an important role in the global carbon budget by affecting the atmospheric concentration of carbon dioxide. It is thus important to quantify the potential impact of climate change on marine primary production. Given the scales at which primary production varies, a satellite measurement approach is necessary. There exist several algorithms which estimate photosynthesis using ocean color-based measurements of phytoplankton biomass, SST, and available irradiance. Previous comparisons of these algorithms indicated considerable variability: if systematic biases were removed, they were within a factor of two of *in situ* carbon uptake measurements. The third Primary Production Algorithm Round-Robin (PPARR3) aims to provide a forum to compare algorithms and to improve their structure and parameterization. This community effort relies on the participation of model developers and users to whom we provide identical input files and whose model output we compile and analyze. Over 15 groups from the U.S., Europe, South America, Japan, and Korea are participating. They use 19 algorithms ranging in complexity from fully wavelength- and depth-resolved ('spectral' models) to simpler depth- and wavelength-integrated algorithms; several of the latter are based on the Vertically Generalized Production Model (VGPM) and others are independently derived (DINT). The first step in PPARR3 is to compare the model output for the annual cycle of 1998. Later parts involve comparison with *in situ* measurements and a detailed comparison of the model derivation of production.



Annual global primary production for each participating model.

The mean global production for 1998 for the 17 models which returned a global estimate was 50 Gt C y⁻¹ and the standard deviation of the mean was 12.5 Gt C y⁻¹ (25%). The model output fell in three bands: **low**, ~35 Gt C y⁻¹ (5 models); **high**, ~65 Gt C y⁻¹ (4 models); and **intermediate**, ~49 Gt C y⁻¹ (most models: 7-8). Ongoing comparisons within PPARR3 will help identify the sources of the divergence and hopefully lead to more consistent results.

Ice Sheet Basal Processes and Ice Paleoclimate Information

Frank Carsey

tel, 818 354 8163; fax, 818 393 6720; email, fcarsey@jpl.nasa.gov

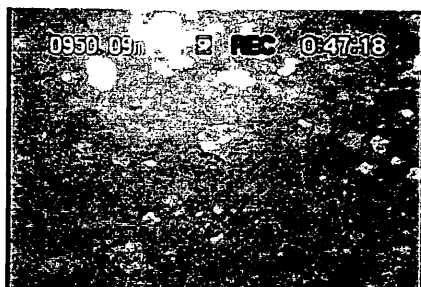
NASA Earth Science Enterprise Strategic Plan Question

What changes are occurring in the mass of the Earth's ice cover?

Scientific Objectives and Motivation. The fundamental scientific objectives of this work are to understand ice sheet basal properties and processes and to determine paleoclimatic history. The motivations of this work stem from recent satellite observations which suggest strongly that the surprising changes occurring in the mass balance of the Antarctic and Greenland ice sheets are a consequence of changes in basal conditions, especially temperature and hydrology. The only sure approach to assessing the cause of changes in basal conditions is through in-situ observations, and, arguably, the best approach to in-situ observations is the deployment of instrumented thermal probes which melt their way down in the ice while acquiring data.

Technical and Programmatic Approach. We have divided the development of the instrumented thermal probe into separate elements, notably the probe itself and its instruments, and we have utilized a number of funding approaches to achieve our goals. To initiate instrument development, we conducted a NASA Earth Science study, in collaboration with Prof. B. Kamb of Caltech, in West Antarctica. Our part of the study was the Ice Borehole Camera, a pressure vessel carrying two cameras into holes drilled by the Caltech group. This project was supported in part by National Science Foundation (NSF), and we plan to work with NSF for the Subglacial Antarctic Lake Exploration program. We conducted the development of a new thermal probe with support from NASA Space Science, Technology, and Earth Science; that work resulted in the first model of a probe, the JPL Cryobot, tested last October. We also have an approved instrument proposal to Space Science and a pending proposal to ESE for a Cryobot deployment.

Results from Antarctic Deployment. The Ice Borehole Camera objectives were to assess the basal accretion of ice on Ice Stream C in West Antarctica, with particular attention to "sticky spots" where subglacial topography led to low basal temperatures. Our findings were that far more accretion ice was present than had been predicted; the mineralogic burden distribution suggested that the rate of freezing had changed considerably over time; and that the accretion cycle may be nearing a shift of behavior. We found on the shoulder of the sticky spot a surprising, shallow, subglacial lake. Below we show sample images from 1 km down in the ice sheet. On the left isolated clasts characteristic of rapid ice growth and on the right regular bands of accreted layers of till characteristic of slower ice growth.



Pacific Climate Variability and Its Impact on the Central California Coastal Upwelling

Yi Chao

tel, 818-354-8168; fax, 818-393-6720; email, Yi.Chao@jpl.nasa.gov

NASA Earth Science Enterprise Strategic Plan Question

What are the consequences of climate and sea level changes and increased human activities on coastal regions?

The coastal ocean off western North America has received considerable oceanographic study because of its fisheries and proximity to large human populations. The region is strongly influenced by the process of coastal upwelling, which occurs along eastern ocean margins when equatorward winds force surface water offshore, drawing deeper water to the surface. The characteristic signature of upwelling is a cool band along the coast, typically tens of kilometers wide, separating from warmer offshore waters by a series of fronts, plumes, and eddies that can extend more than 100 km offshore. In addition to these local features, the central California upwelling system is also influenced remotely by the basin-scale circulation and variability, e.g., El Niño/La Niña and Pacific Decadal Oscillation (PDO).

The long-term objective of this effort is to (1) develop a high-resolution physical model for the central California coastal ocean; (2) nest this high-resolution regional model in a Pacific basin-wide model; (3) develop and refine data assimilation techniques; and (4) validate the model results with *in situ* and satellite observations. Both the basin-scale Pacific model (see Figure 1) and the high-resolution regional model (see Figure 2) will allow us to address the following scientific questions: What are the physical links between the El Niño/La Niña or PDO with the central California upwelling system, and what are their characteristic time and space scales? What alternate physical processes affect the central California upwelling system at these characteristic scales? What are the relative roles of local mesoscale eddies versus remote basin-scale variability in forcing the central California upwelling system?

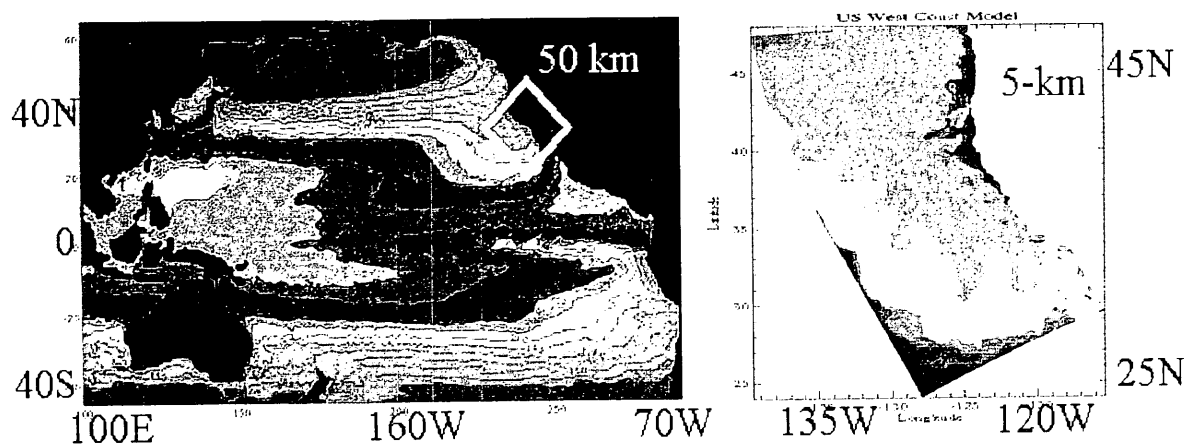


Figure Caption: Snapshots of sea surface temperature simulated by the Regional Ocean Modeling System (ROMS) at 50-km resolution over the Pacific Ocean (left panel) and 5-km resolution off the coast of central California.

Interannual - Decadal Fluctuations in Atmospheric Angular Momentum (AAM) and Sea Surface Temperature (SST): Links among the Earth's Subsystems

Jean O. Dickey

tel, 818-354-3235; fax, 818-393-6890; email, jean.o.dickey@jpl.nasa.gov

NASA Earth Science Enterprise Strategic Plan Question

How is the global ocean circulation varying on interannual, decadal, and longer time scales?

Changes in oceanic heat content and transport play a dominant role in climate processes operating on interannual-decadal time scales, e.g., the El Niño/Southern Oscillation (ENSO) and the Pacific Decadal Oscillation (PDO). In the case of ENSO, feedback between oceanic thermal processes and the local response of the atmosphere is essential to the maintenance of that climate variability mechanism. Poleward propagation of atmospheric angular momentum (AAM) anomalies, originating on the equator and penetrating to high latitudes in both hemispheres in conjunction with the ENSO phenomenon was established by *Dickey et al., [Nature, 1992]*. Since the atmosphere dissipation times are generally on the order of a month or less, it is natural to examine the ocean as a “memory” source for these global scale fluctuations. We confirm this hypothesis by examining monthly sea surface temperature (SST) data from satellite observations beginning in 1982; in addition, we observe a decadal variability (~10-12 years) in both the AAM and SST series (Fig.1). Analyzing Comprehensive Ocean Atmosphere Data Set SST beginning in 1901 (not shown), we observe a longer multidecadal variability of ~ 35 years (the relatively short length of the data sets precludes a robust determination of its period).

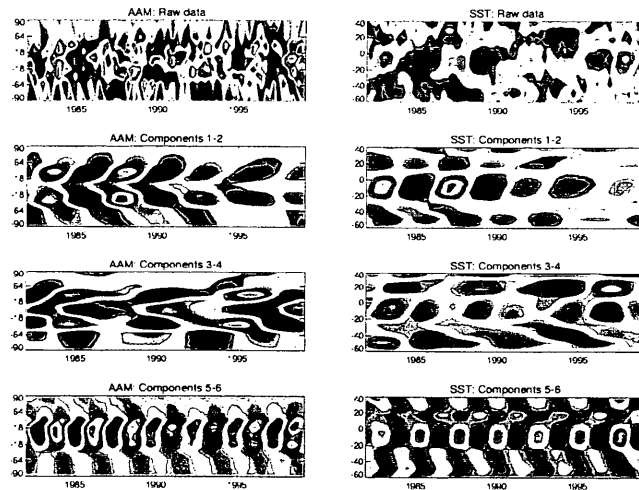


Figure 1. Latitude-time (Hovmoeller) plot of atmospheric angular momentum (AAM, left column) and sea surface temperature (SST, right column) variations. We use the National Center Environmental Prediction reanalysis series integrated over 10 global equal-area latitude belts for the AAM, while the SST is computed for 10 equal-area latitude belts for the Pacific only. The first row displays the raw data of each; the second row entries are the first reconstructed oscillatory pair, comprising the low frequency ENSO component (period ~4-5 years), the third row entries are the nearly decadal pairs (period ~10 years), and the last row contains the quasi-biennial pair. Note that pairs result from multi-channel singular spectrum analysis considering both AAM and SST *Dickey et al., 2002*.

Comparison of ARMAR and TRMM PR Measurements

Stephen L. Durden

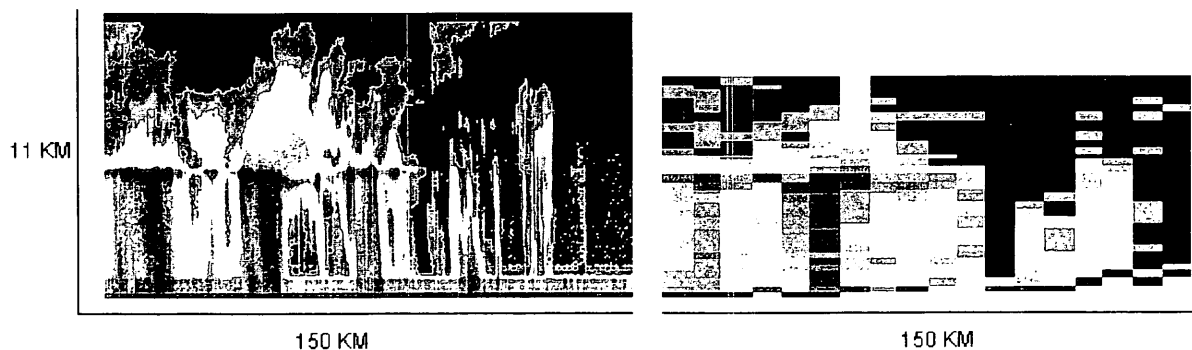
tel, 818-354-4719; fax, 818-393-5285; email, sdurden@jpl.nasa.gov

NASA Earth Science Enterprise Strategic Plan Question

How are global precipitation, evaporation, and the cycling of water changing?

The Precipitation Radar (PR) on TRMM is providing global measurements of precipitation. In an effort to calibrate and validate TRMM measurements several field campaigns were held, in which intensive ground-based and airborne observations were made. The Airborne Rain Mapping Radar (ARMAR) has participated in both part B of the Texas-Florida Underflights (TEFLUN-B) and the Kwajalein Experiment (KWAJEX), collecting large data sets in both experiments. The goal of this work is to use the improved spatial resolution and sensitivity of the airborne sensor to understand resolution and sensitivity effects in the PR measurements. Of particular concern for the PR are the effects of non-uniform filling of its 4.3 km cross-beam footprint. The effects of non-uniform beam-filling (NUBF) have been previously considered theoretically and using ground-based and airborne data. The non-linearity of the relations between rain rate and reflectivity and attenuation result in biases. We address the problem using direct comparisons between ARMAR and PR data.

A total of seven cases with simultaneous, co-located ARMAR and PR observations of rain have been identified. Overall, the PR appears to perform well in detecting and measuring rainfall from space. The PR observations are similar to those of ARMAR, albeit with reduced sensitivity and resolution. The sensitivity biases the maximum altitude of detected storm reflectivity to lower altitudes. The larger footprint can cause biases in observed path attenuation and reflectivity in cases with small, intense convective cells. The classification of rain type provided by the TRMM 2A23 algorithm generally is sound, although some apparent errors were noted, primarily calling convective areas stratiform. This is also likely due to beamfilling effects. The figure below shows vertical slices of reflectivity from the two instruments for a case from KWAJEX (ARMAR left, and PR right). The vertical axis is altitude; the horizontal axis is along-track distance. Reds and purples are areas of highest reflectivity.



Intraseasonal Sea Level Variability from Altimeter Sea Level and Scatterometer Winds

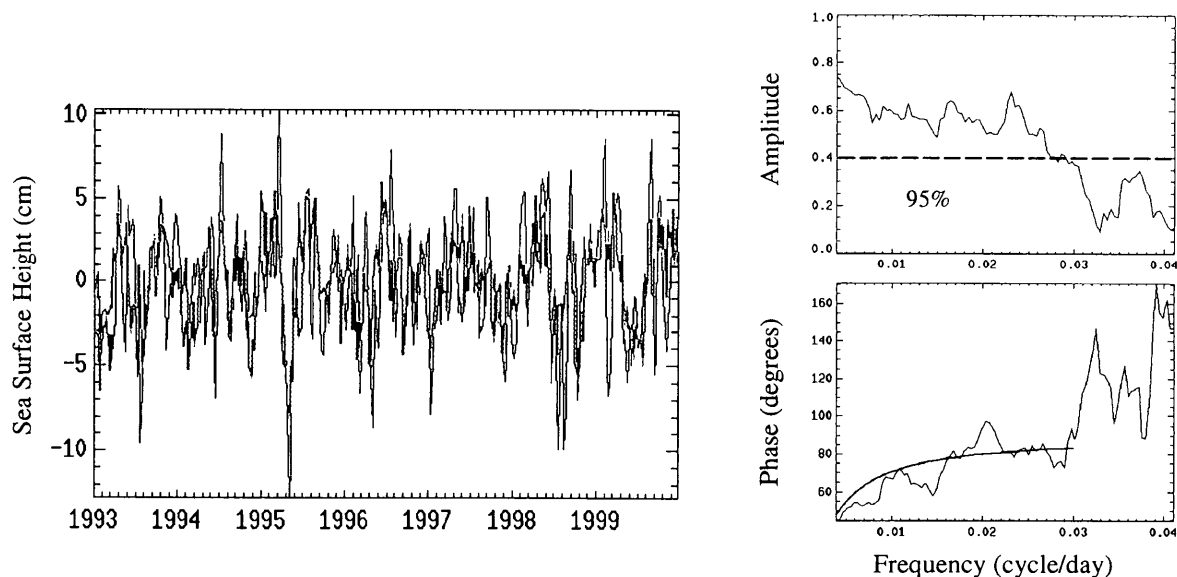
Lee-Lueng Fu

tel, 818-354-8167; fax, 818-393-6720; email, llf@pacific.jpl.nasa.gov

NASA Earth Science Enterprise Strategic Plan Question

How is the global ocean circulation varying on interannual, decadal, and longer time scales?

The intraseasonal variability of the ocean, characterized by time scales less than 180 days and spatial scales larger than 500 km, has been difficult to observe using in-situ methods due to their sparse sampling capability. However, we need to understand this variability in order to address variability of longer time scales because the various scales have both kinematic and dynamic interactions. Seven years' worth of sea level observations from the TOPEX/Poseidon altimeters and wind observations from the ERS-1/2 scatterometers were used to investigate the governing dynamics in the high-latitude regions where the variability is prominent. The basic dynamics can be described by a barotropic vorticity equation, in which the ocean's relative vorticity is balanced by the forcing of wind stress curl and the dissipation at the ocean bottom. Based on this equation, sea level variations were simulated from the wind forcing. The simulations are correlated with the observations at 95% confidence level. A dissipation time scale on the order of 50 days was obtained from the calculations. The phase of the coherence between sea level and wind stress curl also showed dependence on frequency consistent with the dissipation mechanism and its estimated time scales.



Left Figure: Sea level anomalies from the T/P observations (black) and simulation (purple) at 52° S, 260° E in the Bellingshausen Basin.

Right Figure: Coherence amplitude (upper) and phase (lower) between wind stress curl and sea level at 52° S, 260° E in the Bellingshausen Basin. The thick solid line in the lower panel is from theory with 50-day dissipation scale. The dashed line in the upper panel represents the level of non-zero coherence with 95% confidence.

Satellite Data Assimilation

Ichiro Fukumori

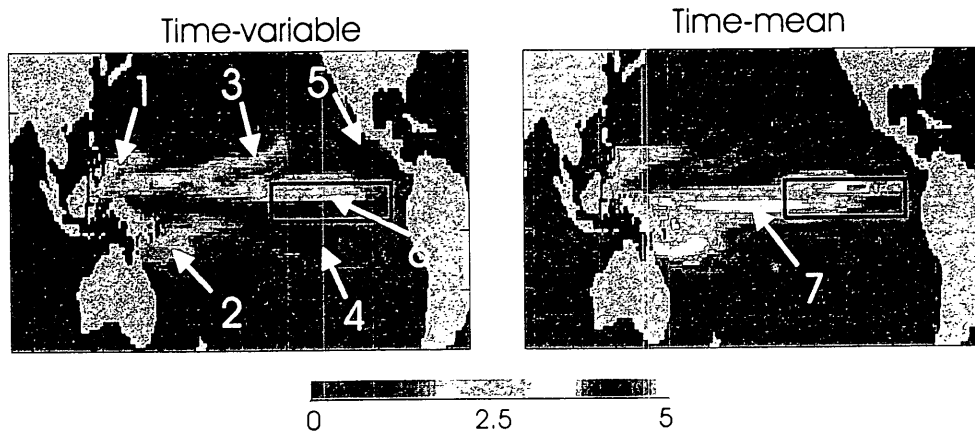
tel, 818-354-6965; fax, 818-393-6720; e-mail, if@pacific.jpl.nasa.gov

NASA Earth Science Enterprise Strategic Plan Question

How is the global ocean circulation varying on interannual, decadal, and longer time scales?

The goal of this research is to infer and to understand the mechanisms of ocean circulation using satellite observations. Using numerical ocean circulation models in conjunction with in situ measurements, satellite observations are dynamically interpolated and extrapolated into a complete three-dimensional description of the ocean.

A high resolution ocean circulation model and data assimilation system have been developed so as to infer global ocean circulation (<http://ecco.jpl.nasa.gov/odap/html/index.html>). The study is part of a consortium entitled "Estimating the Circulation and Climate of the Ocean (ECCO)" (<http://www.ecco-group.org>). Measurements of sea level (TOPEX/Poseidon) and in situ vertical temperature profiles (XBTs and TAO moorings) have been assimilated with the model for the period 1993 to 2001. The assimilation is presently being extended into a near real-time analysis product. Results are being analyzed with particular focus in understanding processes underlying the 1997-1998 El Niño event. The figure below illustrates the origin (and pathway anomalies) of water masses associated with this event. Surface water in the eastern equatorial Pacific that is central to the physics of El Niño ("Niño3" indicated by black box), is traced backwards in time from the end of 1997 (peak of El Niño) to the beginning of 1993. Color indicates relative concentration of this water mass (arbitrary units) per unit area. The source water is traced to separate deep (100-300 m) equatorward flow at the western boundary (1 & 2) and the interior (3 & 4). Near-surface circulation at the eastern boundary (5) and local mixing (6) also contribute to make up the Niño3 water mass. In comparison, the pathway corresponding to the time-mean circulation (right panel) is quite different; the interior and eastern sources are absent, and instead the western boundary source and its flow along the equator (7) dominate the Niño3 water mass. Differences in these pathways are used to test different hypotheses and to understand the nature of the ocean's seasonal-to-interannual changes.



Depth integrated content of water mass in January 1993 that will occupy the surface 10 m layer of "Niño3" (boxed area) in December 1997. The values are equivalent thickness of this water mass in meters.

Large-Scale Oceanic Wave Processes

Roman E. Glazman

tel, 818-354-7151; fax, 818-393-6720; email, reg@pacific.jpl.nasa.gov

NASA Earth Science Enterprise Strategic Plan Question

How is the global ocean circulation varying on interannual, decadal, and long time scales?

One part of my effort - the study of ocean tracer fluctuations and transport caused by large-scale oceanic wave motions - is motivated by the need to improve our understanding of horizontal transport of CO₂, heat, and bio-geochemical quantities and develop physically-based models allowing us to make reliable predictions of the corresponding processes. Joint analysis of TOPEX/Poseidon altimeter and SeaWiFS data facilitated the experimental component of this work. The work also contains significant theoretical and modeling components.

The second part of my effort includes experimental studies of oceanic Rossby waves and other types of quasi-geostrophic motions. These studies were carried out separately for the Pacific equatorial waveguide and for mid-latitude regions. Among the most remarkable results is the finding, illustrated in Fig.1, that Rossby waves of all timescales - from semi- to multi- annual - contain a large meridional component and have a much shorter wavelength than previously thought. These findings have far-reaching implications for our understanding of the role of Rossby waves in ocean dynamics and climate.

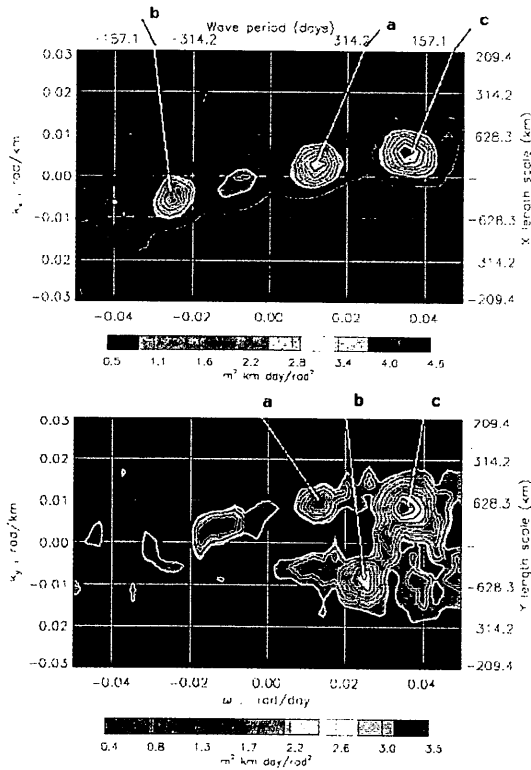


Figure 1: The 2D spectra of SSH variability for Pacific region 170 - 180°E, 20 - 30° N. For each spectral peak, marked by 'a', 'b', etc., we find that $k_y \gg k_x$.

Oceanic Angular Momentum and the Earth's Rotation

Richard Gross

tel, 818-354-4010; fax, 818-393-6890; email, richard.gross@jpl.nasa.gov

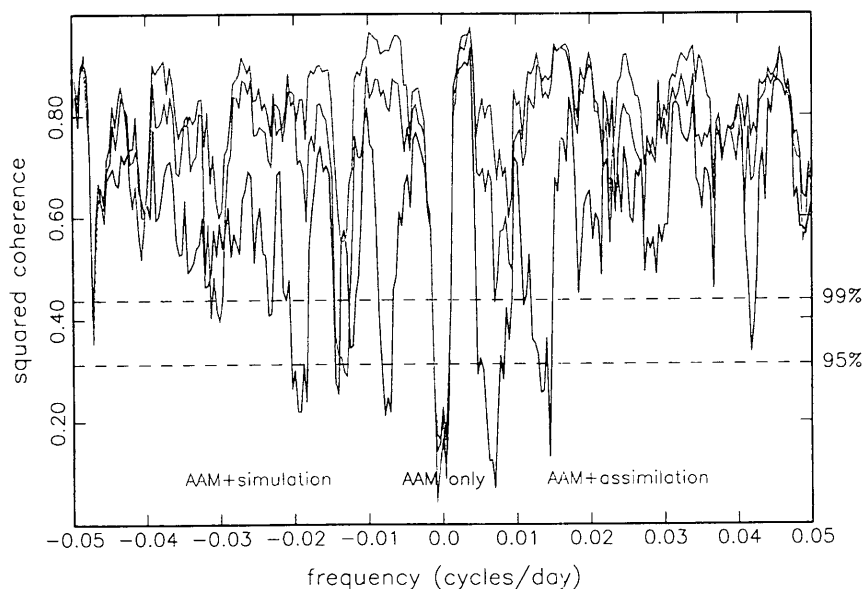
NASA Earth Science Enterprise Strategic Plan Question

What are the motions of the Earth and the Earth's interior, and what information can be inferred about Earth's internal processes?

The angular momentum of the oceans changes as both the distribution of mass within the oceans changes and as the direction and speed of oceanic currents change. Since, in the absence of external torques, the angular momentum of the solid Earth-atmosphere-ocean system is conserved, the changing oceanic angular momentum will cause the solid Earth's angular momentum to change, or, in other words, will cause the Earth's rotation to change. Independent measurements of the Earth's rotation, from which atmospheric effects have been removed, can therefore be used to assess the fidelity of models of oceanic angular momentum.

As part of JPL's participation in the Estimating the Circulation and Climate of the Ocean (ECCO) consortium, ocean models are being used to simulate the general circulation of the oceans. In collaboration with I. Fukumori and D. Menemenlis, oceanic angular momentum (OAM) computed using these models have been computed and are being compared to independently measured changes in the Earth's rotation. The figure below shows the magnitude of the squared coherence between observed polar motion excitation and changes in just atmospheric angular momentum (black), changes in both atmospheric and oceanic angular momentum (red), and changes in both atmospheric and oceanic angular momentum when the OAM is computed from a model that has assimilated TOPEX/POSEIDON sea surface height measurements (blue). The coherence between the observed and modeled excitation is dramatically improved when the oceans' angular momentum is added to that of the atmosphere. Furthermore, the OAM computed using the results of the assimilated model (blue) are clearly more coherent with the observed polar motion excitation than is the OAM computed from the model that did not assimilate sea surface height measurements (red). The results shown here are an example of our use of independent Earth rotation measurements to assess the fidelity of different models of oceanic angular momentum.

COHERENCE OF OBSERVED & MODELED EXCITATION



Using Global Terrestrial GPS Measurements to Unravel the Emerging Altimetric Record of Global Sea-Level Change

Bruce Haines

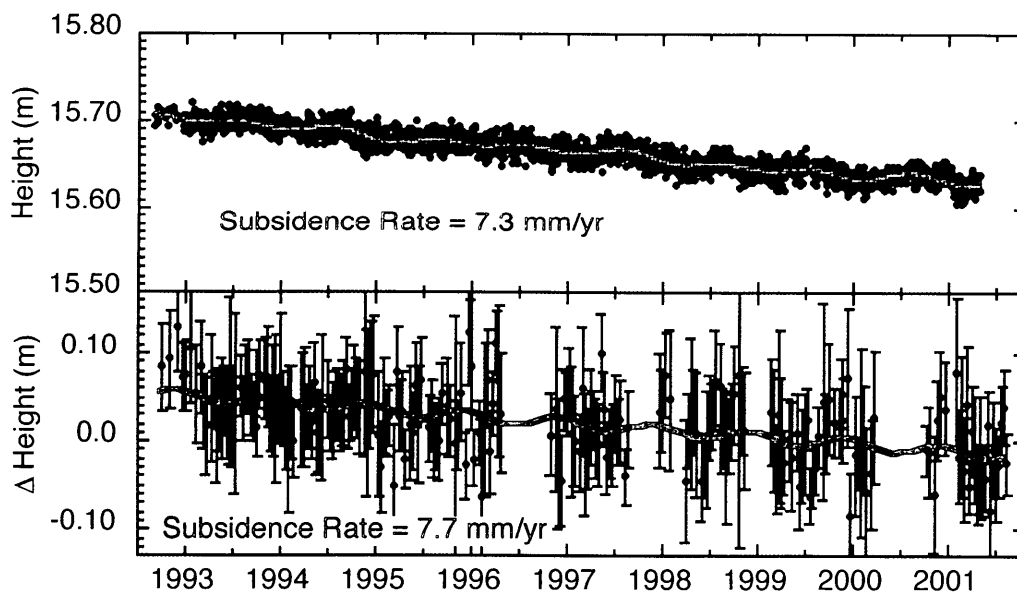
tel, 818-354-0686; fax, 818-393-4965; email, bruce.j.haines@jpl.nasa.gov

NASA Earth Science Enterprise Strategic Plan Question

How well can long-term climatic trends be assessed or predicted?

The Topex/Poseidon (T/P) and Jason-1 era of altimetry (1992–present) has fortuitously coincided with the emergence of GPS as an invaluable scientific tool in both the geodetic and atmospheric sciences. Many of the observations from terrestrial GPS stations (e.g., land subsidence, atmospheric delays) bear directly on the interpretation of the altimetric record of global mean sea level and its constituent measurements. Combined with the rapid growth of the numbers of permanent GPS stations—most notably at coastal and island locations—this has significantly enhanced the potential for exploiting terrestrial GPS as a multi-faceted altimeter calibration tool.

In this study, we are advancing scientific GPS measurements in three areas that are crucial to the calibration of the altimetric sea level record: 1) vertical land motion, 2) columnar water-vapor abundance, 3) and vertically integrated total electron content. The emphasis is on adapting recent innovations in GPS processing to generate long-term quality-controlled time series for each of these measurements. For refining the vertical rates, we focus on the GPS stations collocated with tide gauges used in the calibration exercises. For monitoring the atmospheric variables that influence the propagation of the radar altimeter signal, results from coastal and island stations in the vicinity of the ground tracks will be emphasized. Working with co-investigators, Professors Steve Nerem (University of Colorado) and Gary Mitchum (University of South Florida), our goal is to assimilate the calibration time series and attendant error estimates into the TOPEX/Poseidon and Jason-1 global sea-level record via tide-gauge calibration techniques.



The figure illustrates the subsidence of the sea floor under the Harvest Oil Platform (altimeter calibration site off the coast of Central California). The top panel shows a decade-long time series of daily GPS position estimates. The bottom panel shows the subsidence estimated from the dispersion of the tide-gauge and altimeter sea level (T/P). The agreement is better than 1 mm/yr.





GPS Radio Occultations Coming of Age: Two Spacecraft Launches Add Two New Instruments for Climate Monitoring

George Hajj

tel, 818-354-3112; fax, 818-393-4965; email, George.Hajj@jpl.nasa.gov

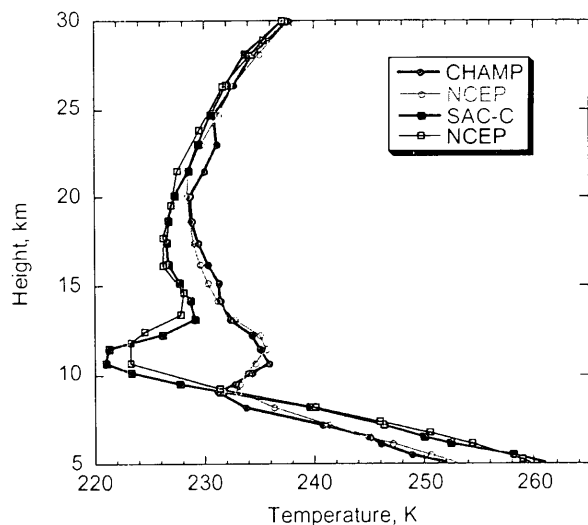
NASA Earth Science Enterprise Strategic Plan Question

How well can long-term climatic trends be assessed or predicted?

Global Positioning System radio occultations are active limb soundings that measure the time delay of a GPS signal propagating through the atmosphere. This time delay can be related to vertical profiles of atmospheric refractivity from which highly accurate profiles of geopotential height, temperature, pressure, and specific humidity are derived. With their global coverage, self-calibrating nature, penetration through clouds, and high vertical resolution, atmospheric radio occultations are coming of age and hold great promise for weather prediction and climate monitoring.

In the year 2000, two satellites, the German CHAMP and the Argentinian SAC-C, were launched carrying a new generation of GPS receivers called "Blackjacks". Developed at JPL, two Blackjacks have been collecting up to 400 occultations daily through much of 2001 and are providing data that complements data derived from other atmospheric sounding techniques. By the spring of 2002, with the launch of the GRACE mission carrying two additional GPS occultation receivers, and when both SAC-C occultation antennas are enabled, it is expected that up to 1200 occultations will be collected daily.

To illustrate some of the features of radio occultations we show two nearby high-latitude occultations from CHAMP and SAC-C in the figure. The two occultations were chosen because of their (1) proximity, within 300km, and (2) quite distinct features. Shown also in the figure are two profiles based on semi-daily analysis from the National Centers for Environmental Prediction (NCEP) interpolated to the locations and times of the occultations. A notable strength of occultation measurements is the ability to resolve the structure of the thermal tropopause with high vertical resolution, whereas the models are effectively smoothing this out. Such high resolution measurements can be of great significance for addressing climate change as a function of height, or the structure and dynamics of the thermal tropopause, which is crucial for understanding the dynamics of transport between the higher troposphere and the lower stratosphere.



Radio occultations can provide an excellent long-term climate record due to their high accuracy (better than 1K between 5 and 35km altitude) and self-calibrating features. Measurements taken today by one mission and a decade later by a different mission can be compared directly without concern for instrumental biases. JPL is making occultation data from CHAMP and SAC-C freely available to the community, reached through the GENESIS data system at <http://genesis.jpl.nasa.gov>.

Sensitivity of Computed Equatorial Ocean Currents to Wind and Data Assimilation

David Halpern

tel, 818-354-5327; fax, 818-393-6720; email, david.halpern@jpl.nasa.gov

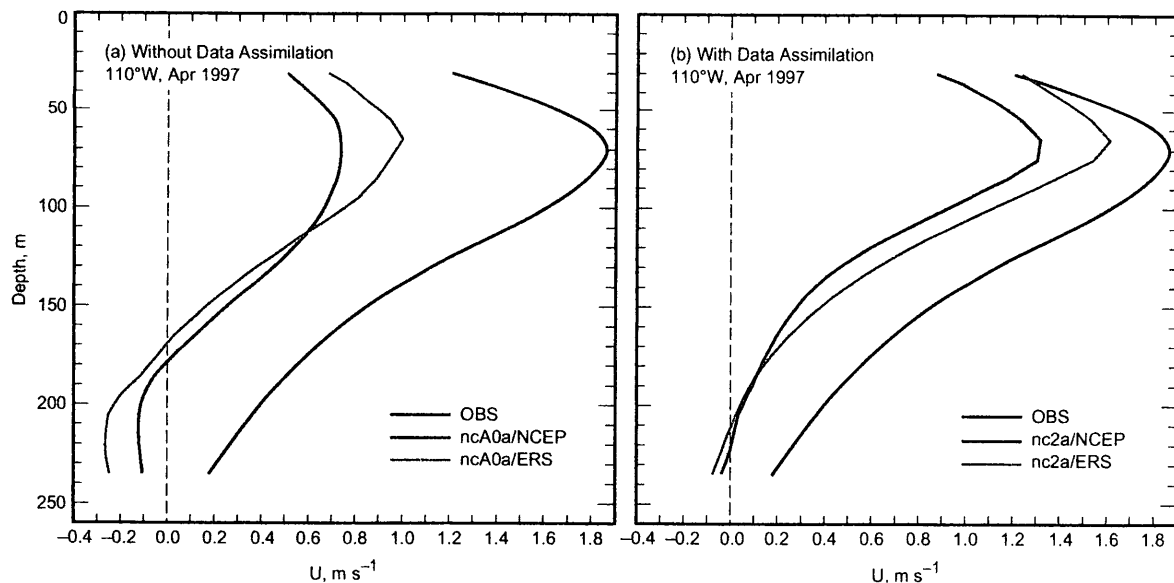
NASA Earth Science Enterprise Strategic Plan Question

How is the global ocean circulation varying on interannual, decadal, and longer time scales?

Assimilation of limited quantities of satellite and in situ observations into numerical models of ocean circulation propagates information throughout the ocean interior. How to accomplish this feat remains a daunting challenge. In collaboration with Dr. David Behringer, National Centers for Environmental Prediction (NCEP), the impact of assimilation of subsurface temperature on upper ocean currents along the Pacific equator is examined for the 1996-1998 period. This interval coincided with the largest El Niño of the XXth century. All simulations were computed at NCEP.

To test the sensitivity of the Geophysical Fluid Dynamics Laboratory modular ocean model, version 3 (MOM3), to wind forcing, two monthly mean wind products were used: NCEP 6-h operational surface wind analyses and European Space Agency European Remote-sensing Satellite (ERS) ocean vector wind measurements. ERS wind stress in the equatorial Pacific was greater than the NCEP wind stress by about 0.01 N m^{-2} . The Pacific Marine Environmental Laboratory Tropical Atmosphere-Ocean moored current measurements at 110°W are used to determine the accuracy of computed currents, even though current measurements have errors.

April is the time of usual occurrence of the annual Kelvin wave along the equator. In April 1997, the Kelvin wave pulse was augmented by the onset of the largest El Niño of the XXth century. This created an anomalously large Equatorial Undercurrent (EUC) core speed in the eastern Pacific. In Figure 1, comparison of left panel with right panel clearly demonstrates the improvement produced by subsurface temperature assimilation in monthly mean computed zonal currents at 110°W for April 1997. Sensitivity of the EUC to zonal wind stress is also displayed in Figure 1, with a stronger EUC associated with ERS winds. Additional improvement is clearly warranted, and experiments will be made with assimilation of satellite measurements of sea surface topography.



Water Vapor in the Lower Stratosphere and Upper Troposphere

Robert Herman

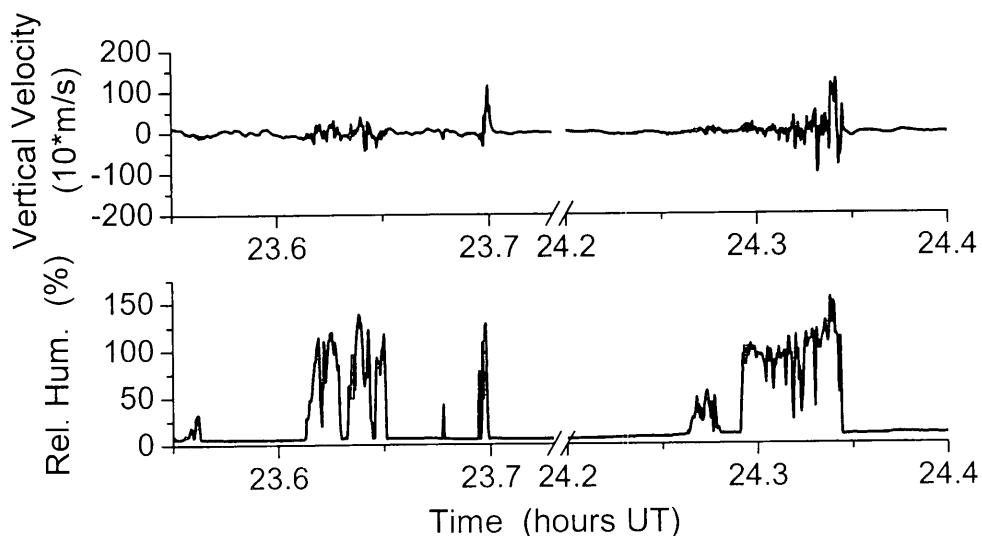
tel, 818-393-4720; fax, 818-354-5148; email, robert.l.herman@jpl.nasa.gov

NASA Earth Science Enterprise Strategic Plan Question

How are global precipitation, evaporation, and the cycling of water changing?

The cycling of water through the Earth's upper troposphere and stratosphere plays a central role in the global energy cycle of the atmosphere. In the vapor phase, water is the dominant greenhouse gas, absorbing outgoing longwave radiation to warm the Earth's surface. It is thought that upper tropospheric water vapor has a substantial radiative impact, despite much lower water content than in the lower troposphere. Another large impact on the energy cycle is latent heat release by water condensation and freezing in clouds.

The Jet Propulsion Laboratory (JPL) Laser Hygrometer (JLH) is a near-infrared diode laser spectrometer for rapid and precise *in situ* measurements of atmospheric water vapor. During the summer of 2001, JLH flew on the NASA DC-8 aircraft platform as part of the NASA Convection and Moisture Experiment (CAMEX-4). JLH measurements directly improve our knowledge of the distribution of water vapor in the upper troposphere. The figure below comes from *in situ* measurements made on September 15, 2001, during CAMEX-4. As the DC-8 flew through Tropical Storm Gabrielle, it encountered strong updrafts, as indicated by the vertical velocity from the Meteorological Measurement System. Within these regions of intense convection, the relative humidity measured by JLH exceeded 100%, indicating supersaturation. The meteorology and cloud microphysics of these supersaturated air parcels are currently under study, in collaboration with Andrew Heymsfield (National Center for Atmospheric Research) and Leonhard Pfister (NASA Ames Research Center). The goal of this study is to better understand water phase transformations in convective cells, which will lead to improved models of hurricanes.



Small-Scale Coastal Eddies and Hazards off California

Benjamin Holt

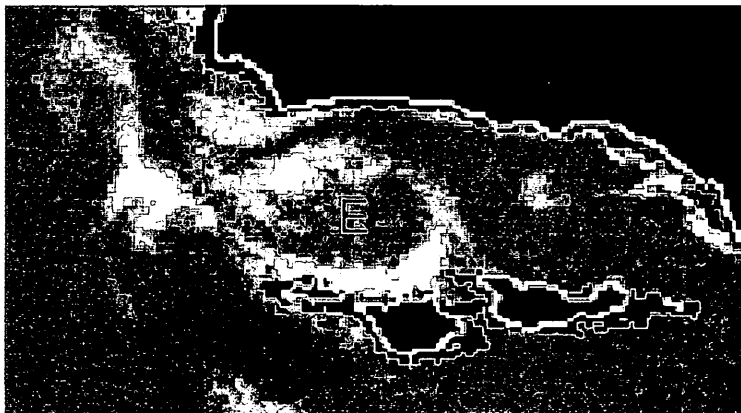
tel, 818-354-5473; fax, 818-393-6720; email, ben@pacific.jpl.nasa.gov

NASA Earth Science Enterprise Strategic Plan Question

How do ecosystems respond to and affect global environmental change and the carbon cycle?

This work seeks to provide a better understanding of productivity, circulation, and pollution in California's coastal waters. The oceanography of the coastal zone is complex and dynamic. The presence of small-scale (< 50 km) processes like eddies, fronts, and internal waves can lead to variable circulation patterns that affect the growth, distribution, and transport of organisms. In particular, the flow fields within these processes can generate convergence zones at the sea-surface, often manifested as slicks, that aggregate organisms and pollutants. The potential impact of small-scale processes on coastal marine ecosystems can be quite significant since these are typically nutrient rich, highly productive regions, and the sites of breeding grounds for many important fisheries. Further, the coastal zone functions as an entry point for a variety of pollutants, via rivers, creeks, storm drains, and sewage pipelines, which can endanger the growth and survival of larval fish and invertebrates. Coastal pollutants can also be derived from natural sources, e.g., hydrocarbons originating from seeps found off the southern California coast in the Santa Barbara Channel and Santa Monica Bay, and spills from ships and drilling platforms which may also affect productivity.

This study will examine adjacent, yet distinct, regions of the California coast, the Southern California Bight, and the central California coast. We will use a variety of satellite sensors including high resolution SAR (from RADARSAT, ERS, and ENVISAT), complemented by satellite-derived ocean color (SeaWiFS and MERIS), and sea surface temperature measurements (AVHRR and AATSR) together with coincident field data (from moorings, drifters, ships, and shore-based HF radar). This suite of data will enable the detection and quantification of under-sampled and poorly described small-scale coastal ocean processes and hazards including eddies, storm water runoff plumes, and hydrocarbon seepage, and an assessment of their bio-geophysical impacts. From our observations, we expect to contribute to the understanding of the seasonal, interannual, and regional variability in the bio-geophysical characteristics of small-scale coastal phenomena as well as provide maps of oil seepage and storm water plumes that are important coastal management tools. This figure shows high chlorophyll-a concentration, derived from SeaWiFS, associated with an eddy in the Santa Barbara Channel on October 27, 1997.



SeaWiFS Chlorophyll-a, mg m^{-3}

Rainfall Observations Using an Airborne Dual-Frequency Radar

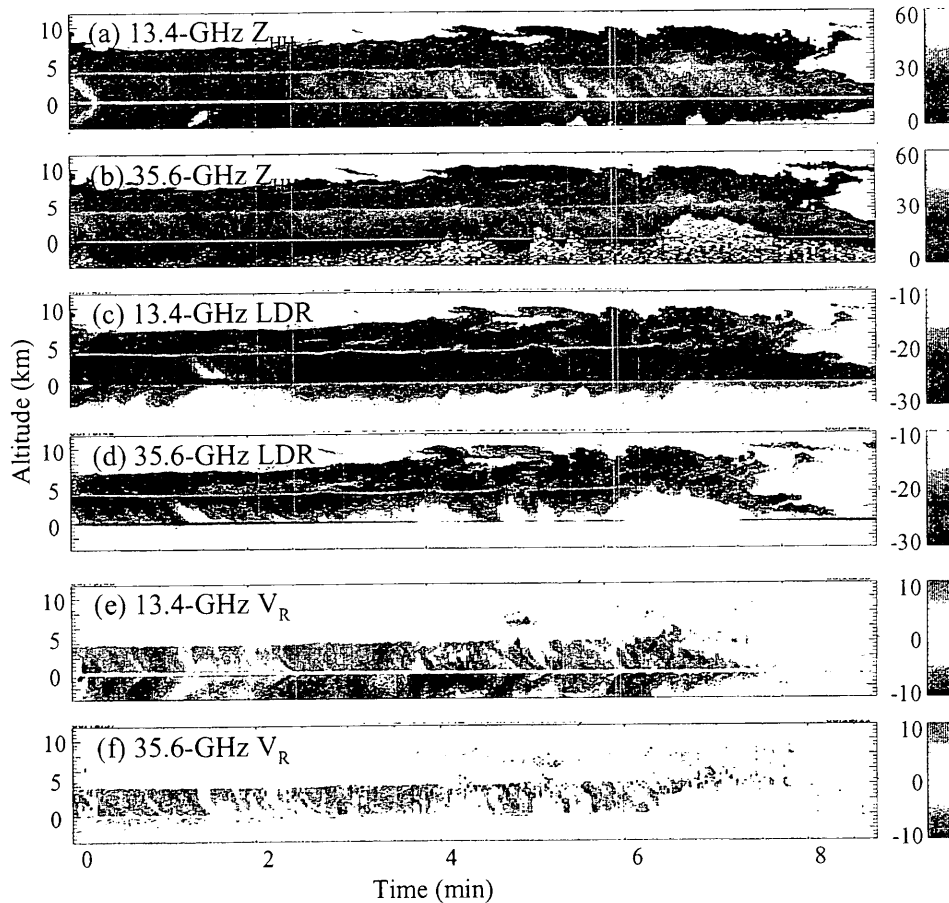
Eastwood Im

tel, 818-354-0492; fax, 818-393-5285; email, eastwood.im@jpl.nasa.gov

NASA Earth Science Enterprise Strategic Plan Question

How are global precipitation, evaporation, and the cycling of water changing?

This research is aimed at the detailed studies of the microphysics and dynamics of rainfall, snowfall, and dense or precipitating clouds in various climatic regimes and geolocations. An airborne dual-frequency (13.4 and 35.6 GHz) scanning radar has been developed for this research. It is capable of measuring vertical structures of rain reflectivity at the two frequencies and at both co- and cross-polarization, as well as the vertical Doppler measurements. During the Fourth Convection and Moisture Experiment (CAMEX-4) off the coast of Florida in August-September, 2001, this radar made detailed rainfall observations over several tropical storms and a hurricane.



This figure shows the rainfall data of Hurricane Humberto acquired on September 25, 2001. The first two panels show the nadir cuts of the 13.4- and 35.6-GHz co-polarized radar reflectivity profiles along the flight path. Detailed structures of both the melting layer and precipitation can be seen in these images. These images also articulate the differences in the rain measurement sensitivities between the two frequencies. The middle two panels are the corresponding LDR profiles. They accentuate the ice particles at the melting layer. The vertical Doppler measurements in the last two panels show the changes in vertical rainfall motion as the plane moved from the older-portion (stratiform) to the younger-portion (convective) of the hurricane.

Postglacial Rebound and Ice Mass Change in Antarctica and Patagonia

Erik R. Ivins

tel, 818-354-4785; fax, 818-354-9476; email, eri@fryxell.jpl.nasa.gov

NASA Earth Science Enterprise Strategic Plan Question

What are the motions of the Earth and the Earth's interior, and what information can be inferred about Earth's internal process?

Understanding the Earth's fluid envelope across a broad spectrum of time scales is essential for isolating the underlying physics driving ocean, atmosphere, and hydrological change. The enormity of the last glacial age, having lowered sea-level by 100-130 meters in growing vast continental ice sheets between about 65,000 to 15,000 years ago, causes the solid Earth to undergo deep motions that have very long time scales (1000 yr. +). Ongoing solid Earth mass exchange processes are called "postglacial rebound" (PGR). It strongly affects long-wavelength signals found in gravity change data, such as detected by LAGEOS, Starlette, Ajisai, and Etalon satellite tracking.

With the launch of CHAMP in 2000, and the GRACE satellite in March of 2002, studies of global climate and sea-level change will begin to reap the benefits an entirely new data set. Gravity data from these missions can be used to better constrain mass change at the surface of the Earth. These satellite data will also be sensitive to PGR, especially at the wavelengths that correspond to ancient ice domes that existed in Scandinavia, Canada, parts of the Arctic oceans, and Antarctica. In areas that are currently ice-covered, such as in Greenland, Antarctica and Patagonia, the gravity signal of PGR interferes with that associated with ongoing ice change. Hence, there is strong motivation for correctly modeling and independently constraining PGR in ice covered regions. Very Long Baseline Interferometry and Global Positioning System (GPS) tracking data along with absolute gravity measurements show that the current rate of vertical rebound of the solid Earth is about 0.1 – 1 cm/yr in the regions that were covered by ancient ice sheets some 15,000 – 22,000 years ago. Radar altimetry over Greenland and Antarctica reveal topographic change signals that are comparable. Is it ice or solid Earth that is changing? The new gravity change data may help Earth scientists sort this question out. One of the key elements of PGR is that it involves the deepest mantle. Hence, the gravitational signature of PGR is inherently of long wavelength. Exactly how much longer depends in a quite sensitive way to the regional structure of mantle viscosity.

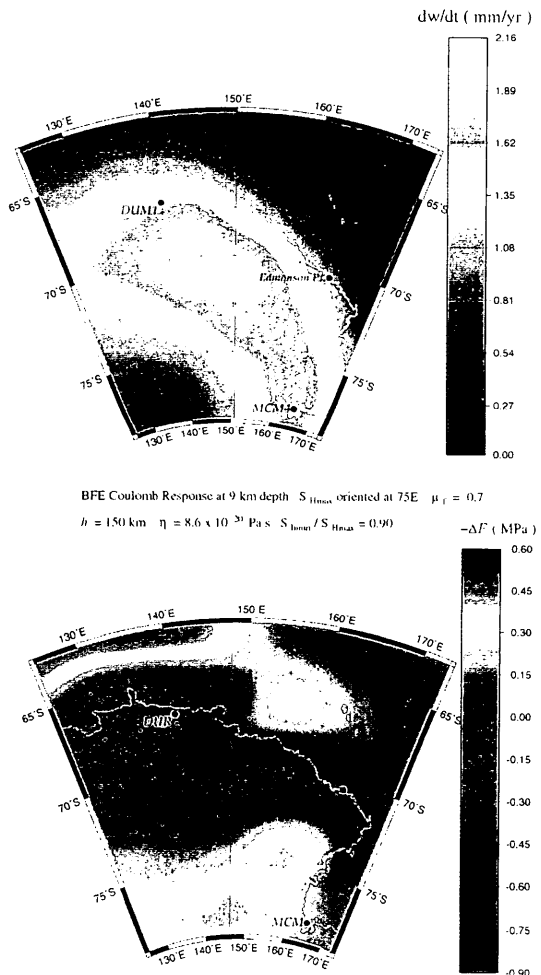


Figure. The top map-view is a predicted PGR uplift rate in George V Land in East Antarctica (permanent GPS tracking stations are also indicated). The bottom frame shows the associated PGR stress field that drives regional seismicity. Note how different the two maps are. (High quality permanent seismic stations are also indicated: 1 MPa = 10 bars).

Positive Mass Balance of the Ross Ice Streams, West Antarctica

Ian Joughin

tel, 818-354-1587; fax, 818-393-3077; email, ian@radar-sci.jpl.nasa.gov

NASA Earth Science Enterprise Strategic Plan Question

What changes are occurring in the mass of the Earth's ice cover?

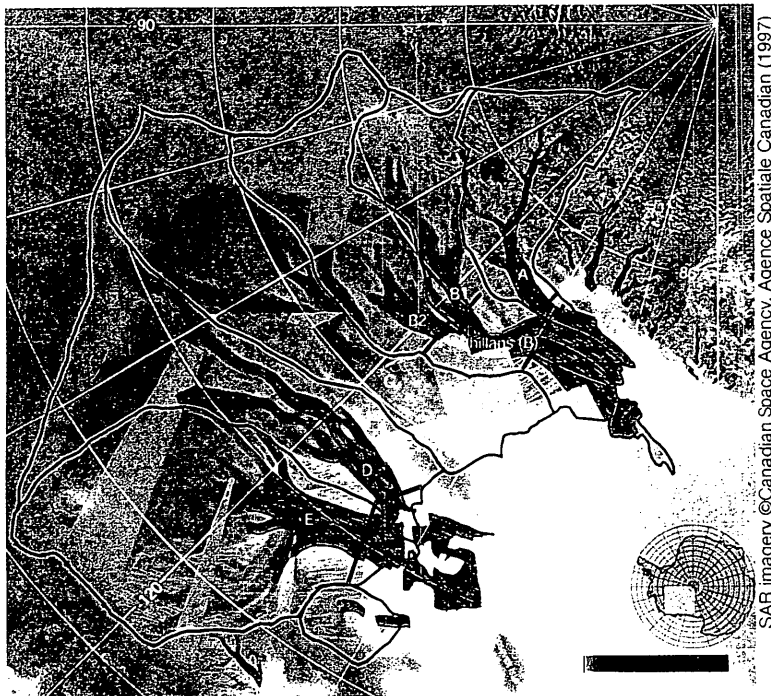


Fig. 1. Ice flow speed (colors) over radar imagery from the RADARSAT Antarctic Mapping Project Mosaic. Flow speed at 100 m/yr intervals is contoured with thin black lines. White vectors show subsampled velocity vectors in fast moving areas. Catchment boundaries for individual ice streams are plotted with thick black lines. Flux gates used in discharge calculations are shown with red lines.

Over the last several decades there has been concern regarding the possibility that the marine-based West Antarctic Ice Sheet might collapse within the next several centuries, raising sea level by 5-6 meters. This concern was supported by evidence that this part of the ice sheet was thinning. I have used ice velocity measurements from synthetic aperture radar (SAR) to reassess the mass balance of the Ross Ice Streams, West Antarctica. This study found strong evidence for ice sheet growth (+26.8 Gton/yr), in contrast to earlier estimates indicating a mass deficit (-20.9 Gton/yr). Average thickening is equal to ~25% of the accumulation rate, with most of this growth occurring on Ice Stream C. Whillans Ice Stream, which was thought to have a significantly negative mass balance, is close to balance, reflecting its continuing slow-

down (~23% deceleration of Whillans Ice Stream from 1974 to 1997). The overall positive mass balance may signal an end to the Holocene retreat of these ice streams.

Unlike earlier results that relied on relatively sparse *in situ* measurements of ice-flow velocity, the revised estimate was based on the interferometrically derived velocity field shown in Figure 1. These velocity data along with surface topography data were used to determine the catchments for individual ice streams (thick black lines in Figure 1). Ice discharge flux was estimated through a "gate" located near the grounding line at the downstream end of each catchment (red lines Figure 1). The total accumulation for the catchment area above each gate was determined by integrating gridded accumulation data. The difference between the accumulation (input) and discharge (output) gives the mass balance for each catchment.

Seasonal Sea Ice Deformation, Growth, and Production

Ron Kwok

tel, (818) 354-5614; fax, (818) 393-3077; email, ron.kwok@jpl.nasa.gov

NASA Earth Science Enterprise Strategic Plan Question

What changes are occurring in the mass of the Earth's ice cover?

The RADARSAT Geophysical Processor System (RGPS) produces measurements of ice motion and estimates of ice thickness using repeat synthetic aperture radar (SAR) maps of the Arctic Ocean. From the RGPS products, we can compute the net deformation and advection of the winter ice cover using the motion observations, and the seasonal ice area and volume production using the estimates of ice thickness. The contrast in the behavior of the sea ice over the winters of 1996/1997 and 1997/1998 is quite remarkable. The second winter is of particular interest because it coincides with the SHEBA field program. The deformation (Fig. 1) and the ice volume produced by the ice cover during the two years are very different. Over a domain covering a large part of the Western Arctic Ocean ($\sim 2.5 \times 10^6$ km²), the net divergence of that area during the six months of the first winter is 2.7% and the second winter is more than 9.3%. In a sub-region where the SHEBA camp is located, the net divergence is almost $\sim 38\%$ compared to a net divergence of the same subregion of only $\sim 9\%$ in 1996/97. The deformation, its variability and net, created a much larger volume of seasonal sea ice than the earlier winter. The net seasonal ice volume production is 1.6 times (0.38 m vs 0.62 m) that of the first year. In addition to the larger divergence, this part of

the ice cover advected a longer distance toward the Chukchi Sea over the same time span. The total coverage of multiyear ice remained almost identical at $\sim 2.08 \times 10^6$ km² or 83% of the initial area of the domain. The final locations of these sub-regions reflect the mean atmospheric pressure pattern and ice motion field of the Arctic Ocean over the winter. During the SHEBA year, the Beaufort high pressure cell is centered north of the Chukchi Sea resulting in strong zonal winds and westward ice motion north of the Alaska coast. Subregion 1, where the SHEBA ice camp is located, advected far west toward Wrangel island. The weaker high pressure cell centered farther south during the first year resulted in a much weaker ice motion pattern in the southern arm of the Beaufort Gyre.

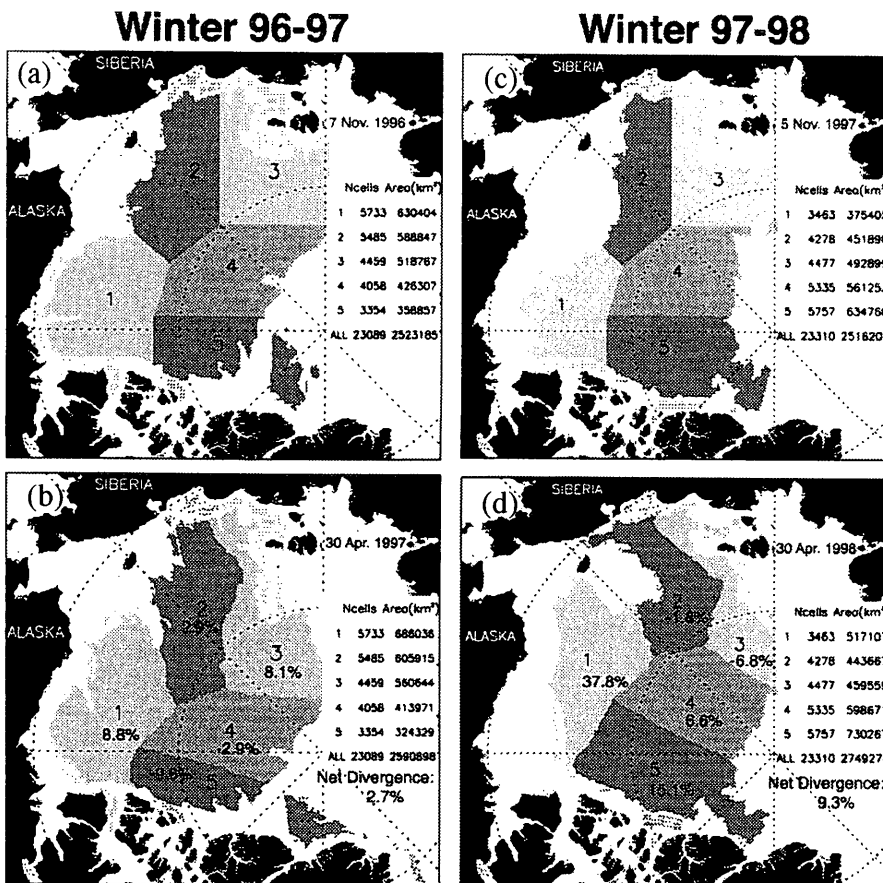


Figure 1. The spatial coverage of the five sub-regions (S_1 - S_5). (a) November 7, 1996. (b) April 21, 1997. (c) November 5, 1997. (d) April 30, 1998. The areas of the sub-regions and the number of cells in each sub-region are also shown.

Hurricane Studies With HAMSR

Bjorn H. Lambrigtsen

tel, 818-354-8932; fax, 818-393-4619; email, lambrigtsen@jpl.nasa.gov

NASA Earth Science Enterprise Strategic Plan Question

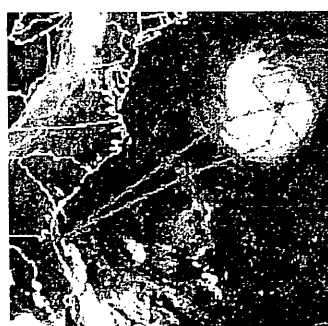
How can weather forecast duration and reliability be improved by new space-based observations, data assimilation, and modeling?

Tropical cyclones (e.g., hurricanes) play an important role in the global heat budget and moisture cycle by transporting moisture into the upper troposphere, generating cirrus and cumulus clouds and transporting heat to mid latitude. Hurricanes are also among the potentially most destructive weather systems, particularly during landfall. Much effort has therefore recently been devoted to hurricane research, with the general objective of gaining a better understanding of the processes involved and the specific objective of improving hurricane landfall forecasting. During the last decade a series of NASA field campaigns, known as the Convection and Moisture Experiments (CAMEX), have been conducted to study tropical convective processes. The most recent in the series, CAMEX-4, was carried out as a joint effort with other government agencies in Florida between August 15 and September 25, 2001.

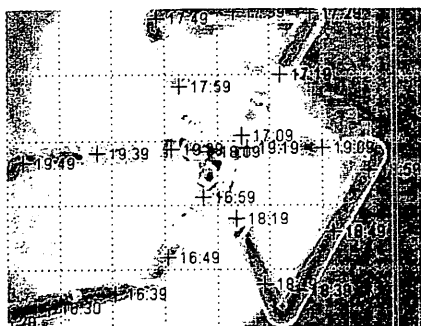
The High Altitude MMIC Sounding Radiometer (HAMSR) is a microwave atmospheric sounder recently developed by JPL under the NASA Instrument Incubator Program. Using new technology, it is a small but accurate instrument that is well suited for hurricane studies. Operating with 25 spectral channels in the 50 - 190 GHz region, it provides measurements that can be used to infer the 3-D distribution of temperature, water vapor, and liquid water in the atmosphere, even in the presence of clouds. Parameters related to scattering from ice particles aloft as well as precipitation can also be inferred. During CAMEX-4, HAMSR was mounted in a wing pod of a NASA ER-2 research aircraft, which operates at an altitude of 65,000 feet and therefore can overfly hurricanes. HAMSR participated in a number of sorties during CAMEX-4, and a large amount of data was collected and is currently being processed and analyzed. The objectives of this effort are:

- Provide calibrated brightness temperatures to other CAMEX researchers
- Use those, along with observations from other instruments, to infer scattering parameters
- Derive temperature, water vapor and liquid water profiles
- Study horizontal and vertical moisture transport in and around intense convective systems.

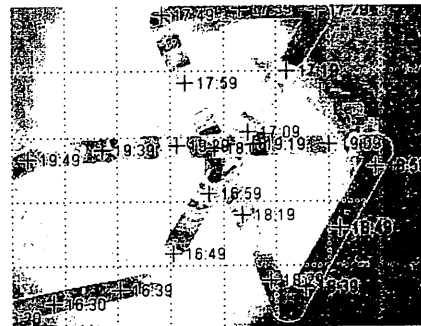
The analysis effort is currently in its initial stages.



Hurricane Erin, 9/10/01



a. 50.3 GHz channel



b. 166 GHz channel

HAMSR data from hurricane Erin (9/10/01), showing the observations in two channels. Fig. a shows data from a transparent temperature channel. The ocean surface appears cold (blue) due to low emissivity. The eye of the hurricane is visible (note that it moves between successive legs of the flight). Fig. b shows data from a transparent moisture channel. Pink areas represent warm moisture 2-4 km above the surface (the surface itself cannot be seen). Blue areas represent regions that appear extremely cold due to scattering, primarily from high altitude graupel.

Interannual to Decadal Variation in Tropical-Subtropical Exchange Processes

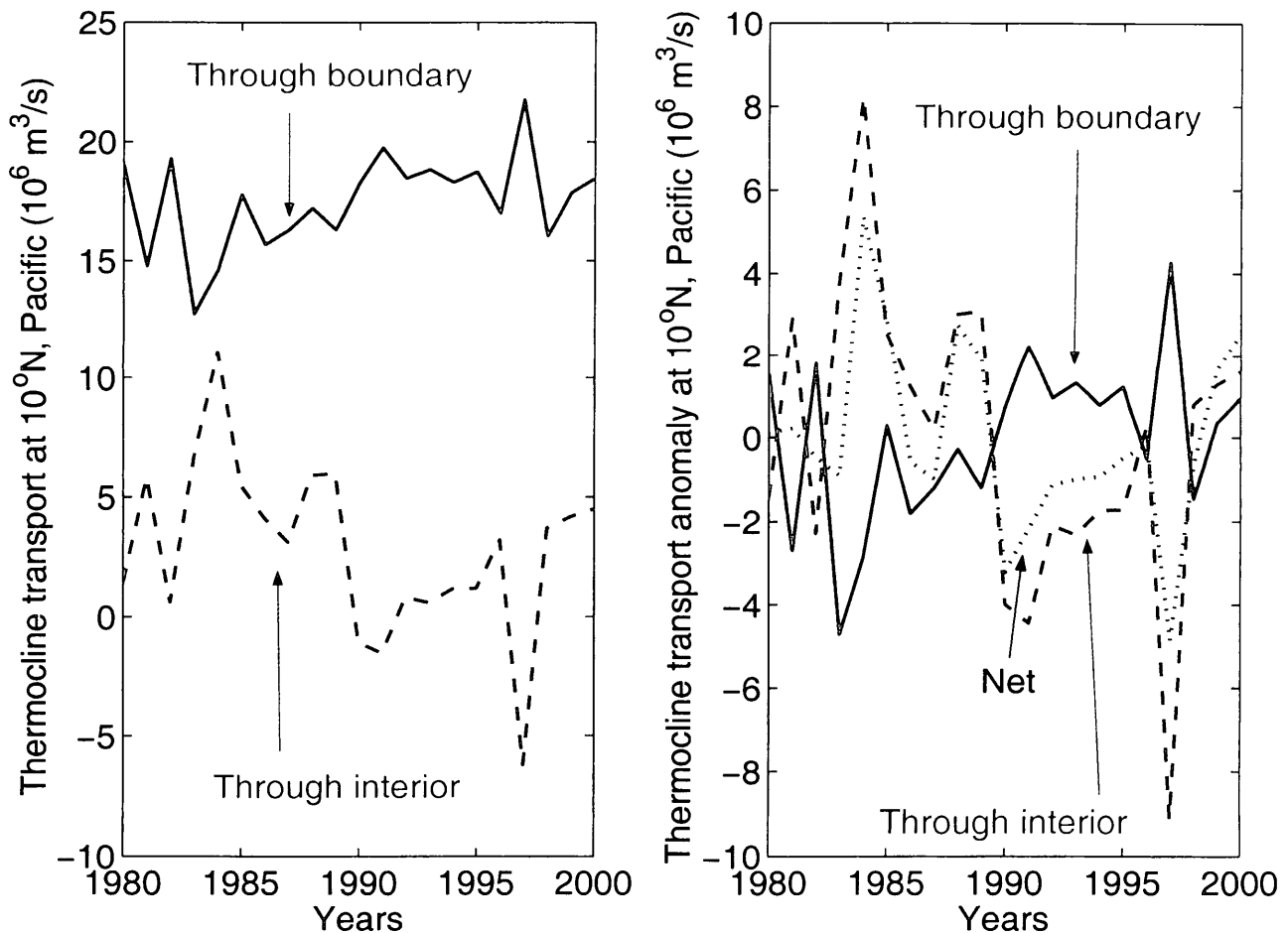
Tong Lee

tel, 818-354-1401; fax, 818-393-6720; email, tlee@pacific.jpl.nasa.gov

NASA Earth Science Enterprise Strategic Plan Question

How is the global ocean circulation varying on interannual, decadal, and longer time scales?

My research focuses on estimating and understanding oceanic variability on interannual to decadal time scales using ocean models, data, and their optimal combination through advance data assimilation methods. More information can be found on <http://ecco.jpl.nasa.gov> (project) and <http://eyres.jpl.nasa.gov> (assimilation product). Highlighted here is a finding with regard to the interannual to decadal variation of tropical-subtropical water mass exchange which has important implication to decadal modulation of ENSO. Waters subducted in the subtropical North and South Pacific arrive at the tropics either through the interior or low-latitude western boundary currents (LLWBC). On average, LLWBC transport is larger than and re-enforces that of the interior (left panel). On the interannual to decadal time scale, however, the variation of LLWBC transport in the 1980s is smaller but counteracts that of the interior (right panel). The net transport of thermocline water (having the same sign as the interior) to the equator is stronger in the 1980s than the 1990s. This is associated with (not shown) a weaker easterly trade and a lower meridional overturning circulation (less poleward Ekman flow and less equatorial upwelling), less poleward heat divergence, and a warmer upper tropical ocean in the 1990s. The picture is consistent with a very recent analysis based on observations (McPhaden and Zhang, *Nature*, Feb. 2002).



Sea Surface Salinity Remote Sensing

Fuk K. Li

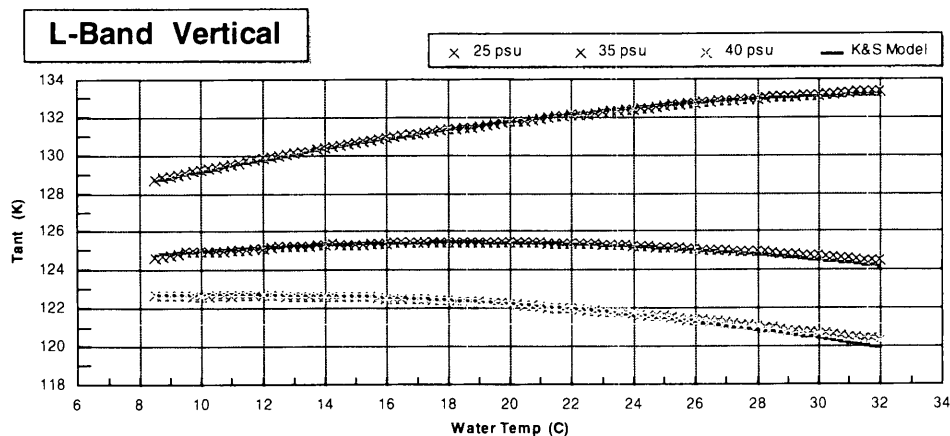
tel, 818-354-2849; fax, 818-393-0068; email: fuk.li@jpl.nasa.gov

NASA Earth Science Enterprise Strategic Plan Question

How is the global ocean circulation varying on interannual, decadal, and longer time scales?

The objective of this research is to develop a microwave remote sensing technique for global sea surface salinity measurements from space. In October and November 2001, L- and S-band radiometer brightness temperature measurements from a salt-water pond were made as a function of salinity and temperature using the Jet Propulsion Laboratory (JPL) Passive/Active L-/S-band (PALS) microwave instrument. The purpose of these measurements was to verify the accuracy of current saltwater microwave emission models. Having accurate microwave emission models for the L-band emission from the ocean is necessary for future satellite missions to measure sea surface salinity as proposed in the NASA Goddard Space Flight Center/JPL Aquarius mission.

Most of the measurements were taken at fixed salinity levels of 25, 35, and 40 psu over a temperature range of 9° C to 32° C. These measurements cover most of the range expected in the oceans to be measured by the Aquarius instrument. All the averaged L-band measurements from five different days, at vertical polarization, are shown as the colored points in the following figure. The Klein and Swift (K&S) model data are shown as the solid black curves. The rms difference between the average curves and the K&S model is 0.1 K, which corresponds to a salinity error < 0.2 psu. This demonstrates the excellent stability of the PALS measurement system.



The conclusion from this set of controlled measurements is that over most of the range of salinity and temperatures observed in the ocean, the K&S model, with minor corrections, will provide accurate predictions for the L-band emission from the ocean. This result then forms a sound basis for future spaceborne missions to accurately measure ocean salinity.

The next step of this research is to conduct a field campaign with flights on the NCAR C-130 in July 2002 with the PALS instrument to determine the sensitivity of water brightness temperatures to surface roughness for open ocean conditions.

Ocean-Atmospheric Interaction in Climate Change

W. Timothy Liu

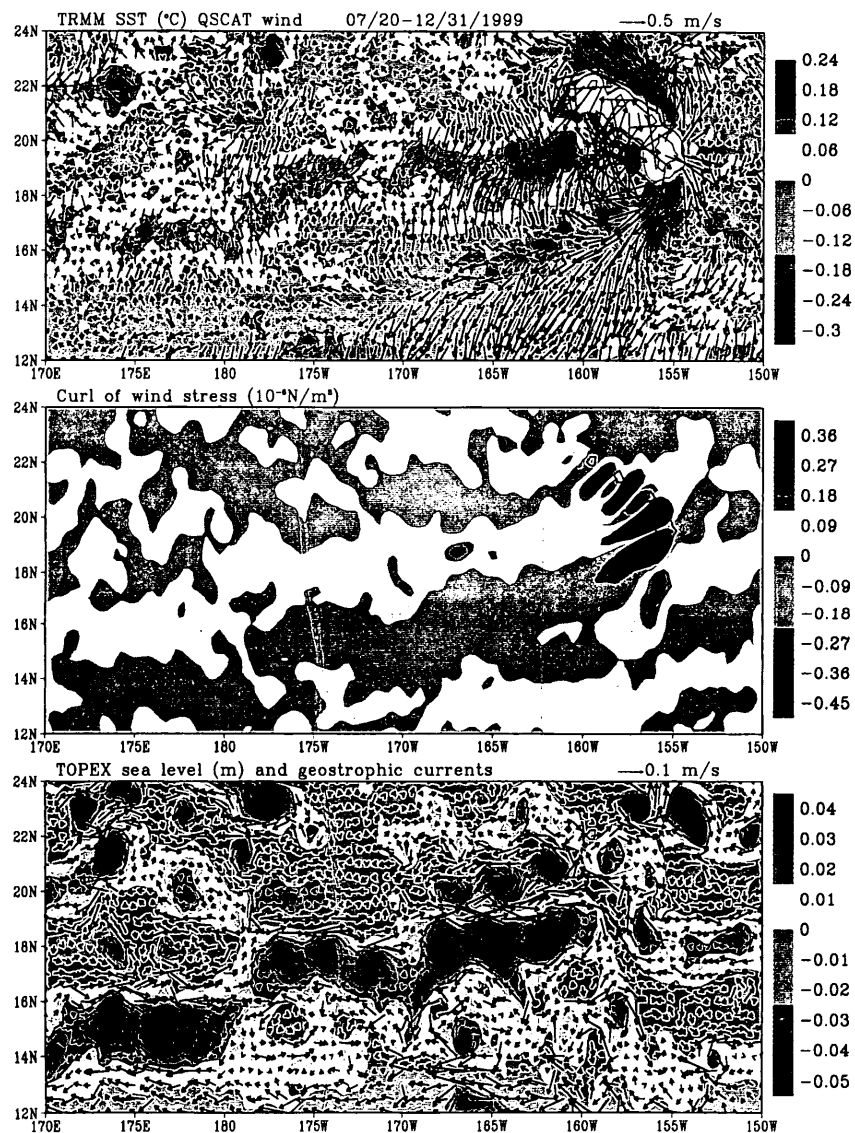
tel, 818-354-2394; fax, 818-393-6720; email, liu@pacific.jpl.nasa.gov

NASA Earth Science Enterprise Strategic Plan Question

How well can transient climate variations be understood or predicted?

Our major scientific contribution in 2001 is in understanding tropical ocean-atmosphere interaction. We revealed a long break in the westward Pacific Trade Wind and North Equatorial Current, stretching more than 3000 km from the Hawaiian Islands to the western Pacific. An eastward current marked by higher sea surface temperature, higher cloud liquid water and surface wind convergence was found to lie between positive and negative sea level deviations (shown in the figure). The effect of the Earth's rotation on wind convergence generates positive and negative wind stress curl, which drive ocean circulation. The break may be triggered by the islands but is sustained by positive ocean-atmosphere feedback. We also showed that vertical mixing in the sheared atmospheric boundary layer contributes significantly to the surface wind field when sea surface temperature is not sufficiently warm to meet the deep convection threshold, as over the tropical instability waves. Multiple advanced statistical techniques were also applied to scatterometer winds to characterize and to understand the wide spectra of temporal and spatial modes of tropical circulation systems.

We continued our long-term effort to apply various space-based sensors to characterize and to understand atmospheric and oceanic phenomena. We continue to improve the estimation of space-based wind, thermal and hydrologic forcing on the ocean, and to provide on-line access to these data through our data system (<http://airsea-www.jpl.nasa.gov/seaflex>).



Microwave Temperature Profiler (MTP) Support for CAMEX-4

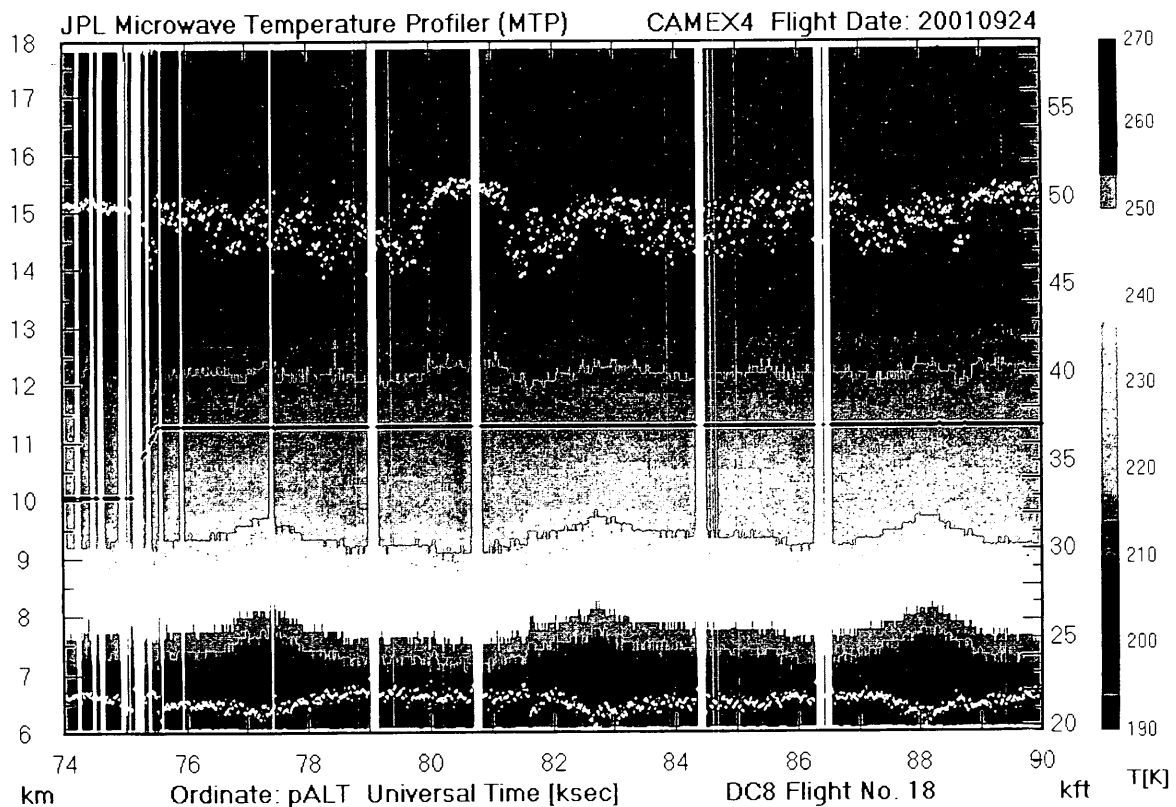
M. J. Mahoney

tel, 818-354-5584; fax, 818-354-4341; email, michael.j.mahoney@jpl.nasa.gov

NASA Earth Science Enterprise Strategic Plan Question

How can weather forecast duration and reliability be improved by new space-based observations, data assimilation, and modeling?

During August-September 2001, Microwave Temperature Profilers (MTPs) flew aboard the NASA DC-8 and ER-2 research aircraft in support of the CAMEX-4 campaign. By observing the natural thermal emission from molecular oxygen, MTPs can retrieve a vertical temperature profile along an aircraft's flight track. This information helps scientists to understand the effect of diabatic heating and cooling -- which is associated with water phase changes -- on hurricane dynamics. Together with moisture and wind, temperature is one of the primary state variables needed to initialize numerical weather prediction models, and hence to understand a model's ability to track hurricanes and predict their intensity at landfall.



The figure above shows the temperature field (color scale to the right) measured by the DC-8 MTP while making three passes over Hurricane Humberto on September 24, 2001. The black trace is the DC-8 pressure altitude (km on left axis, kft on right axis), and the white dots show the tropopause altitude. It is clearly evident that the MTP sees the expected temperature increase in the eye of this hurricane, which the DC-8 flew through at ~77.5, 82.5 and 88.5 ks UT. These measurements will be invaluable for testing hurricane-forecast models.

Geodetic Signatures of Intraseasonal – Interannual Changes in the Climate System

Steven L. Marcus

tel, 818-354-3477; fax, 818-393-6890; email, steven.marcus@jpl.nasa.gov

NASA Earth Science Enterprise Strategic Plan Question

How well can transient climate variations be understood and predicted?

A dominant source of climate variability on interannual time scales is the El Niño / Southern Oscillation (ENSO), which originates in the tropical Pacific but has global consequences. Recently, increasing attention has been given to understanding and predicting the coupled atmosphere / ocean processes which govern the onset of ENSO events. In particular, intraseasonal (~75-day) variations in surface wind stress over the West Pacific (WPAC) have been shown to generate baroclinic Kelvin waves, which propagate into the central equatorial Pacific where they may impact the evolution of the ENSO cycle. In this work, we identify geodetic signatures of some of the processes involved in the triggering of ENSO events.

The solid Earth continually exchanges angular momentum with the atmosphere and oceans, leading to small but measurable changes in its rotation rate and consequently in the length-of-day (LOD). We used space-geodetic LOD data to demonstrate significant coherence between Earth rotation and WPAC wind stress at intraseasonal periods, thereby identifying a potential geodetic precursor to El Niño events (Fig. 1). This interpretation is supported by Fig. 2, which shows the correlation of intraseasonal (60-100 day) filtered amplitude series with Nino3, a measure of sea-surface temperature (SST) anomalies related to ENSO. Significant correlations with WPAC wind stress, LOD, AAM (atmospheric angular momentum), and the LOD-AAM residual are obtained at SST lags of 5-8 months. Since the LOD-AAM residual is representative of oceanic angular momentum, its correlation with Nino3 SST confirms its link with the Kelvin-wave process outlined above, and highlights the ability of space-based geodesy to "see" into the oceans.

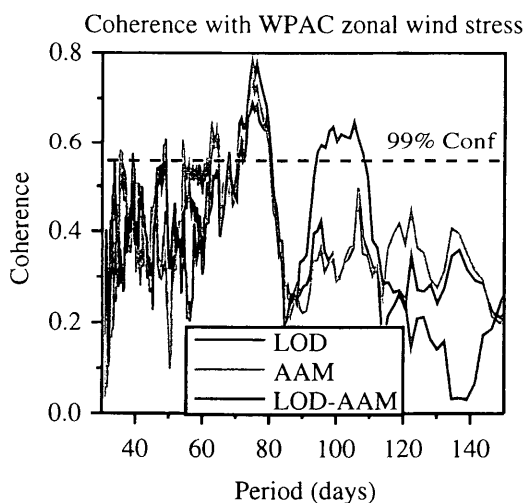


Fig. 1. Coherence of LOD, AAM and their residual (LOD-AAM; representative of oceanic angular momentum) with WPAC wind stress; note significant peaks for all three quantities at periods near 75 days.

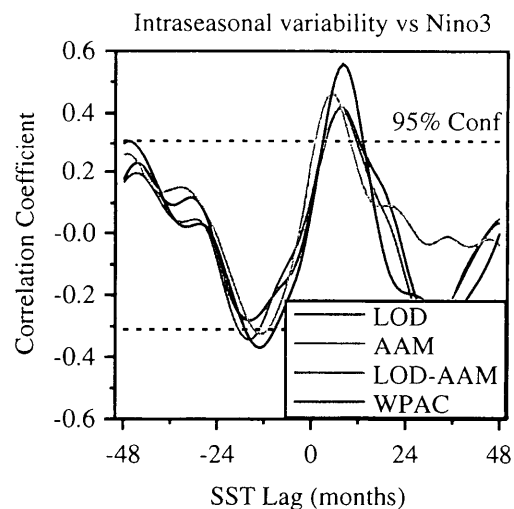


Fig. 2. Correlation of 60-100 day amplitude series with monthly Nino3 SST anomalies. The shorter lead time for the LOD-AAM residual reflects its direct link to oceanic processes. Data interval spans 1976-1999.

Sea Ice and Global Ocean Circulation

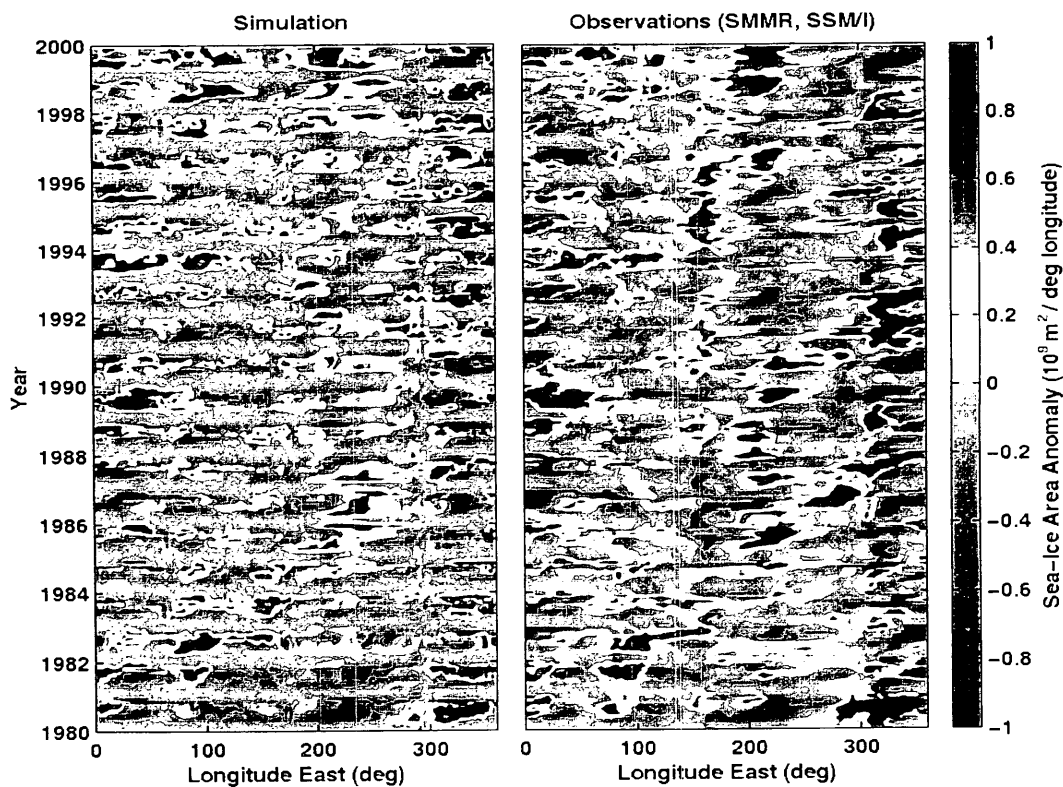
Dimitris Menemenlis

tel, 818-354-1656; fax, 818-393-6720; email, menemenlis@jpl.nasa.gov

NASA Earth Science Enterprise Strategic Plan Question

How is the global ocean circulation varying on interannual, decadal, and longer time scales?

Sea ice interacts with regional and global climate in many ways: it affects surface albedo, ocean convection, polar lows, and ocean/atmosphere exchanges of heat, freshwater, momentum, and various biogeochemical constituents. In particular, an increasing number of modeling studies have shown that the consideration of realistic sea-ice processes often leads to significant improvement in the representation of high-latitude uptake of anthropogenic CO₂ and other transient tracers. Conversely, distributions and properties of sea ice are affected by wind, temperature, salinity, and waves. Our objective is to study and quantify the role of sea ice and high-latitude ocean processes on interannual to decadal climate variability. The analysis will be based on a coupled sea-ice, global-ocean model that is made consistent with satellite and in-situ observations using data assimilation. In a preliminary step, a global-ocean, general circulation model was coupled to a dynamic/thermodynamic sea ice model and used to simulate oceanic and sea-ice circulations. The figure below compares results from this simulation to passive microwave data. The differences between the simulation and the observations will be used to constrain uncertain model parameters and hence produce a realistic representation of the coupled sea-ice, global ocean system, which in turn will be used to study high-latitude climate processes.



Integrated Instrumentation for the JPL Cryobot: The Dust Sensor

Claus Tilsted Mogensen

tel, 818-393-3298; fax, 818-393-6720; email, claus.mogensen@jpl.nasa.gov

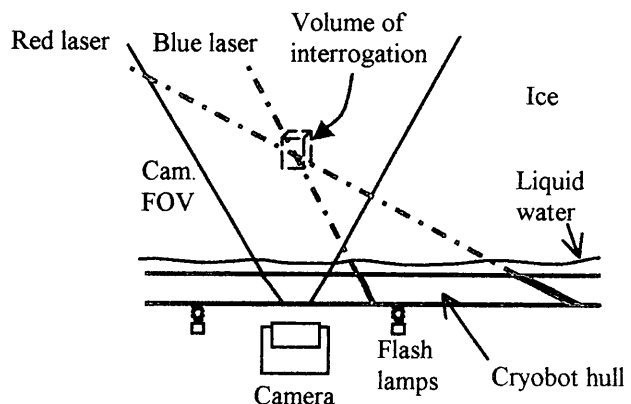
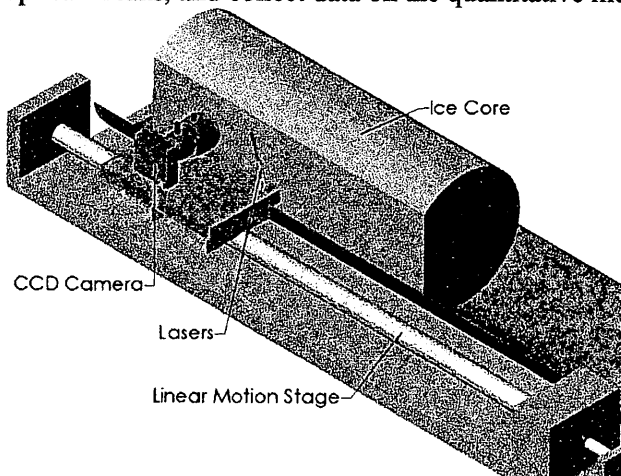
NASA Earth Science Enterprise Strategic Plan Question

What changes are occurring in the mass of the Earth's ice cover?

Scientific Objectives and Motivation. The fundamental scientific objectives of this work are to design, test and integrate an optical dust sensor for the JPL Cryobot, a new in situ thermal probe that melts its way down in ice while acquiring data from, among other instruments, the dust sensor. The long-term objectives of the Cryobot are to acquire data in ice sheets of Earth, the ice caps of Mars, and the icy shell of the Jupiter moon Europa. While still advancing the technology of the basic vehicle, we are addressing the integration of scientific instruments to obtain data on the undisturbed ice adjacent to the Cryobot as well as the melt water it produces. This way a fully implemented instrumentation package is capable of interrogating a possibly pristine environment in a completely non-destructive way.

Technical and Programmatic Approach. Scientific observations of the adjacent ice can be carried out by analytical optical means through analysis of scattered and emitted light; this is the approach we are taking now. A particularly simple yet important observational technique is the analysis of dust inclusion in the ice by way of Lorenz-Mie type scattering. The instrumentation is new, but it is in fact largely a variation on systems used to monitor ice core dust levels during ice core operations as well as systems used to monitor aerosols in the atmosphere. Thus, we are developing a design for an optical dust sensor that is compatible with implementation on a Cryobot, and the indications are that a quite sensitive device can be built that can resolve dust on a very fine vertical scale (perhaps 0.1 mm). In short, the dust sensor works by illuminating the ice using a laser oriented about 45° from normal to the Cryobot and detecting scattered light with a CCD camera oriented normal to the Cryobot at a location in which the laser beam is at a distance of about 50 mm from the Cryobot.

Results and Preparative Field Work. We are now at the point of assembling an optical dust sensor for laboratory ice analysis. We have not yet verified our calculations for the scattered intensity as a function of dust loading, laser wavelength, and geometry, which is crucial. Our approach is to bring the dust sensor to the National Ice Core Laboratory in Denver, Colorado to verify its capability to measure dust levels in archived ice from the Greenland and Antarctic ice sheets. Specifically, our intention is to: verify geometry and wavelength predictions for light scattering by dust in ice, assess the performance of light sources and cameras for this environment, develop data on signal to noise for dust in ice using optical means, and collect data on the quantitative measure of dust in ice.



Timing and Scales of Arctic Sea Ice Albedo Transitions Observed with RADARSAT-1 Data and RGPS Products

Son V. Nghiem

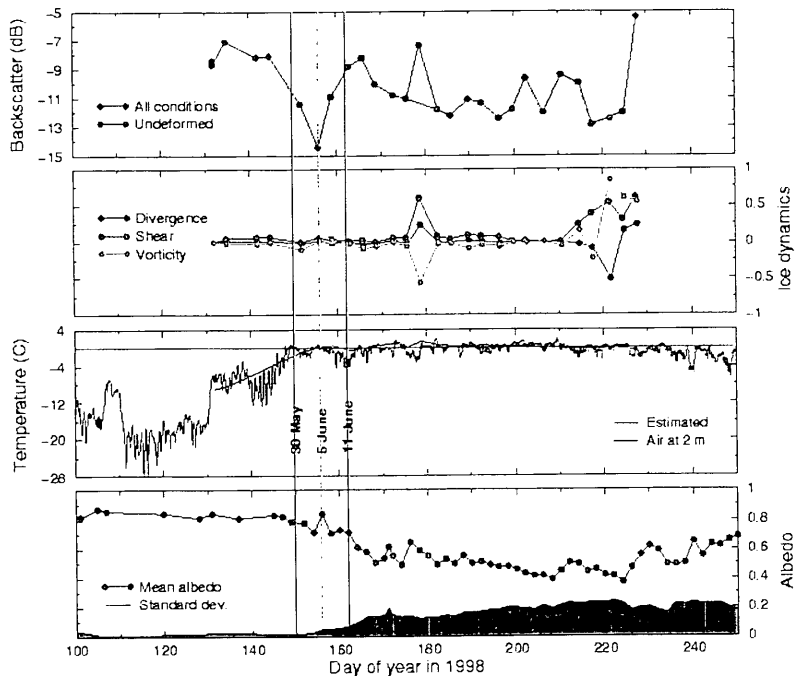
tel, 818-354-2982; fax, 818-393-3077; email, son.v.nghiem@jpl.nasa.gov

NASA Earth Science Enterprise Strategic Plan Question

What changes are occurring in the mass of the Earth's ice cover?

The ice-albedo feedback mechanism plays a key role in the heat and mass balance of the ice and upper ocean in the Arctic that affects the global climate system. We propose to derive both timing and scales of Arctic sea ice albedo transitions using RADARSAT-1 data from the Arctic Snapshot program and sea ice products from the RADARSAT Geophysical Processor System (RGPS). This is done in conjunction with field results from SHEBA (Surface Heat Budget of the Arctic Ocean) and C-ICE (Collaborative Interdisciplinary Cryospheric Experiments) together with Climate System Model GCM (General Circulation Model) calculations.

Timing of the backscatter switches is determined from the RADARSAT time-series, and the correlation between the backscatter switches and albedo changes together with heat flux balance and other parameters measured from SHEBA are studied. We extract RGPS time-series for more than 370 Lagrangian cells around SHEBA including backscatter, incidence angle, divergence, vorticity, and shear together with ancillary data such as wind speed, wind direction, and air temperature. The figure below shows results at the SHEBA location over the time period of spring-summer 1998. The top panel presents backscatter signatures for the SHEBA cell of 10 km by 10 km including deformed and undeformed sea ice defined with an absolute value of the divergence below 0.2. As observed, ice deformation can have a strong effect on local backscatter



which needs to be separated from thermodynamic effects to study the relationship to sea ice albedo. The second panel is for ice deformation. Air temperature in the third panel indicates the first significant backscatter decrease is caused by melting temperature. The period of the “backscatter dip” between 5/30-6/11/1998 was the snow melting period with a slight drop in albedo. After 6/11 following the backscatter dip, albedo decreased strongly due to pond formation. Thus, backscatter can identify the timing of the albedo transition.

Corals Impacted by Interannual and Decadal Climate Variability

William C. Patzert

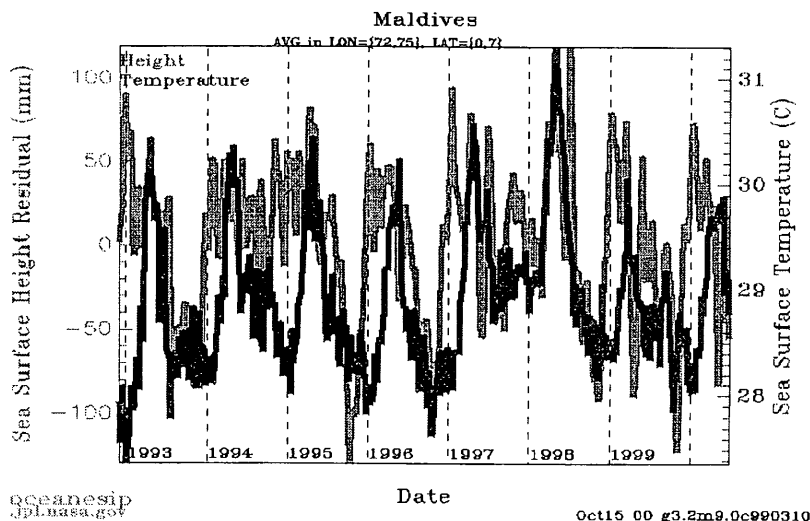
tel, 818-354-5395; fax, 818-393-6720; email, wpatzert@pacific.jpl.nasa.gov

NASA Earth Science Enterprise Strategic Plan Question

What are the consequences of climate and sea level changes and increased human activities on coastal regions?

During the 1997/1998 El Niño to La Niña climate event, public concern and scientific attention was riveted on extensive coral bleaching throughout the tropics. Internationally, >29% of all reef sites surveyed experience significant bleaching, with a total of 20% destruction of live coral. These El Niño- and La Niña- induced events clearly demonstrated that corals are highly sensitive to natural interannual climate variability, as well as continuing short-term anthropogenic environmental abuses. Using NASA/CNES TOPEX/Poseidon sea level height data, NOAA's Advanced Very High Resolution Radiometer sensor derived sea surface temperature products and REEF CHECK *in situ* data, the development of the '97-'98 "bleaching explosion" was mapped temporally and spatially in all tropical oceans. (See the figure below that documents the unusually warm sea surface temperatures and high sea levels that caused an 80% coral mortality throughout the Indian Ocean's Maldives Islands in the spring of 1998.)

Recent imagery from TOPEX/Poseidon shows that when the El Niño switched to the 1998 La Niña, the entire Pacific Ocean switched to a new phase of the multi-year Pacific Decadal Oscillation (PDO). The emergence of this very strong pattern could indicate a dramatic switch in the PDO from the El Niño friendly "warm phase" of the past 20 years to a more La Niña friendly "cool phase" in the coming few decades. This new pattern has caused anomalously warm ocean temperatures and higher than normal sea levels in the tropical Western Pacific which has recently triggered serious coral bleaching in SE Asian waters and over much of Australia's Great Barrier Reef. These results are providing a new dimension to our understanding of coral sensitivity to past, present, and future interannual, as well as decadal, climate variability.



Importance of the Indonesian Throughflow (ITF) to Understand and Predict El Niño/La Niña Events in the Pacific

Claire Perigaud

tel, 818-354-8203; fax, 818-393-6720; email, cp@pacific.jpl.nasa.gov

NASA Earth Science Enterprise Strategic Plan Question

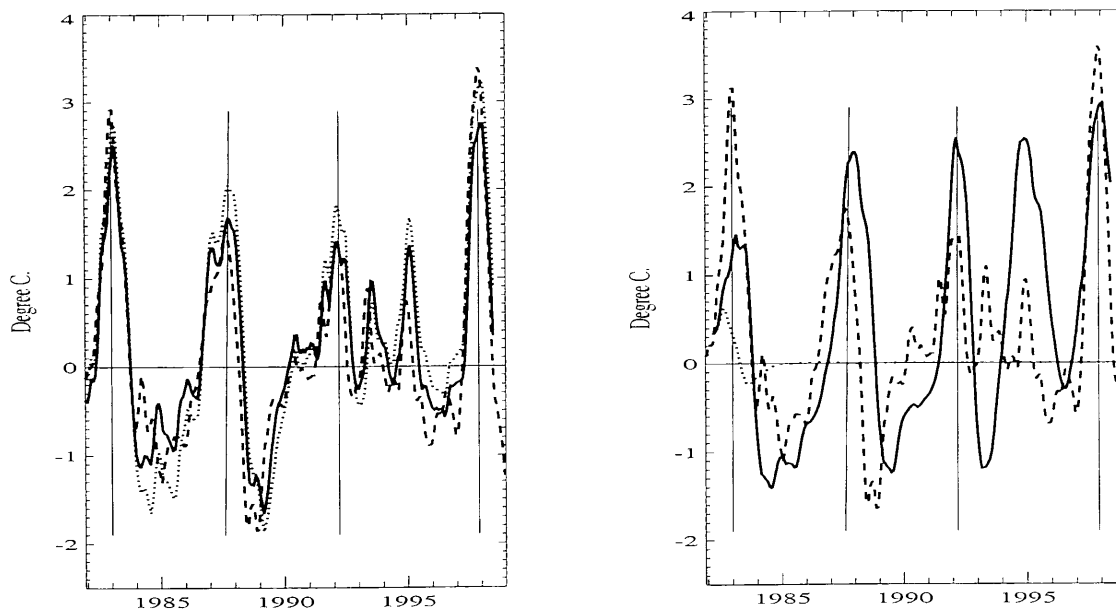
How well can transient climate variations be understood and predicted?

An ocean-atmosphere model forced by observed winds is able to reproduce the observed El Niño/La Niña events very well. This is true whether the model is submitted to closed conditions at the boundary between the Pacific and the Indian Ocean (without ITF) or to conditions that vary in time (with ITF) according to the estimates that can be obtained from TOPEX satellite and in situ data.

Used in a prediction context (fully free of data), the ocean-atmosphere model without ITF simulates SST anomalies that depending on initial conditions, are damped (like in the example below) or oscillating by several °C, but the predicted warm (El Niño) and cold (La Niña) events are not at all in phase with the actual events. When data are used to prescribe the ITF only, the model is able to predict the wind, the ocean currents and the SST which agree reasonably well with reality over these 20 years.

These very successful results mean that it is worth using data and coupled ocean/atmosphere models to detect processes that have been neglected up to now and to improve our ability to understand and simulate the connections between these neglected processes and the actual evolution of our climate.

The figure below compares SST anomalies in the eastern tropical Pacific between 1980 and 2000 from data (dashed lines) and from a model (plain or dotted lines). The model is integrated in time either in a forced context (left panel: the model is forced by observed winds) or in a prediction context (right panel: the winds, ocean currents and SST are predicted by the model). The dotted lines represent the model without ITF, the plain lines represent the model with ITF.



Ionospheric Calibration for Ocean Altimeters

Xiaoqing Pi

tel, 818-354-4257; fax, 818-393-5115; email, xiaoqing.pi@jpl.nasa.gov

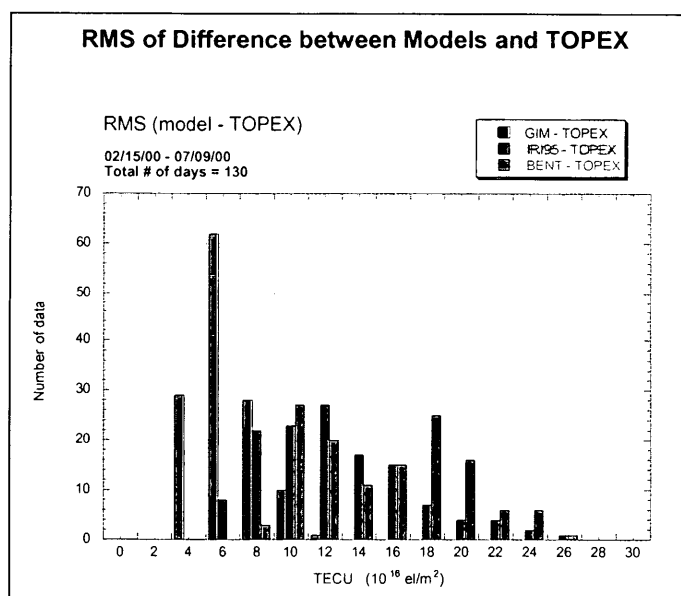
NASA Earth Science Enterprise Strategic Plan Question

How is the global ocean circulation varying on interannual, decadal, and longer time scales?

Sponsored by the U.S. Navy and NASA, an ionospheric calibration process has been continuously operating at the Jet Propulsion Laboratory to support the Navy's altimetry mission of GEOSAT Follow-On (GFO) since 1999. This process routinely collects GPS data from a global GPS network composed of hundreds of ground receiver stations, processes the data to obtain ionospheric observables, and produces sub-hourly (15-minute) time-series of global ionospheric maps (GIM) within 24 hours on a daily basis. The mapped total electron content (TEC) has been applied to remove altimeter signal delay caused by the ionosphere along the satellite orbit tracks above oceans, helping to increase the altimetry accuracy significantly. The global ionospheric maps have also been contributed to the further development of ionospheric models and space weather research.

The accuracy of ionospheric mapping technique is affected by a lack of observing sites in oceanic regions. This is compromised in GIM by temporal and spatial interpolations of TEC measurements over the continents in a Sun-fixed geomagnetic coordinate system. Such a frame is favorable to the reduction of interpolation errors, because the ionosphere is mainly driven by the solar EUV radiation production and dynamical processes in the ionosphere are mostly controlled by the geomagnetic field.

The accuracy assessment is routinely conducted by comparing GIM with TEC measured using the TOPEX altimeter, which operates with dual frequency radio signals that also allow ionospheric TEC retrievals along the TOPEX/Poseidon orbit tracks. In addition, empirical ionospheric models, such as the International Reference Ionosphere (IRI) and Bent models, are also compared with TOPEX-derived TEC as a reference. The figure included in this page gives an example showing the root-mean-squares of difference between models (GIM – data driven mapping technique, IRI95, and Bent) and TOPEX measurements. The comparisons include data of about 5 months (~20,000 data values) in a solar maximum year when absolute TEC values can be in the order of 200 TECU at tropical latitudes. The statistics indicate that the data-driven GIM technique overwhelms the empirical models.



The Impact of Volcanic Emissions on the Regional Environment

Vincent J. Realmuto

tel, 818-354-1824; fax, 818-393-6962; email, vince.realmuto@jpl.nasa.gov

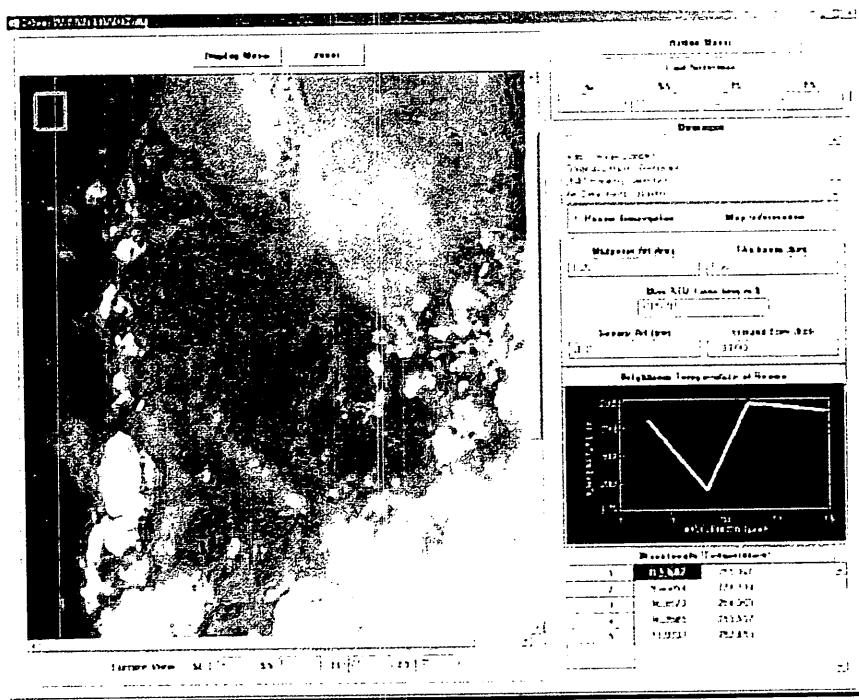
NASA Earth Science Enterprise Strategic Plan Question

What are the effects of regional pollution on the global atmosphere, and the effects of global chemical and climate changes on regional air quality?

This research project, which is led by Dr. Peter Mouginis-Mark of the University of Hawaii, is funded through the EOS Interdisciplinary Study (IDS) Program. The objective of this research is to observe and characterize the impact of volcanic sulfur dioxide (SO_2) emissions on the regional environment. To accomplish this objective, we will analyze data collected by the Advanced Spaceborne Thermal Emission and Reflection Spectrometer (ASTER), Moderate-resolution Imaging Spectrometer (MODIS), and Multi-angle Imaging Spectroradiometer (MISR) over Kilauea Volcano (Hawaii) and Masaya Volcano (Nicaragua). Both of these volcanoes exhibit virtually continuous emission of SO_2 , which is rapidly converted into sulfate aerosols. The acidic atmospheric conditions generated by the sulfate aerosols are the agents of the impact the volcanoes have on the regional environment.

The detection of the Kilauea and Masaya plumes from space will be complicated by humid atmospheric conditions. To address this concern, a new water vapor correction procedure has been developed and tested using MODIS Direct Broadcast data acquired over Hawaii. This procedure calculates a correction factor at each pixel of the image data, thus accommodating spatial variations in the distribution of water vapor in the atmosphere. The water vapor correction strategy will be generalized to correct for ozone absorption and emission at $9.5 \mu\text{m}$, a critical spectral region for the differentiation of SO_2 and sulfate aerosols.

The figure at right is an example of the graphic user interface to the SO_2 estimation procedure. This interface allows users to collect radiance data from specific areas within the scene and enter the parameters required by the radiative transfer code to recover an estimate of SO_2 concentration from the observed radiance.



Satellite Radar Observations of the Mass Balance of Polar Ice Sheets

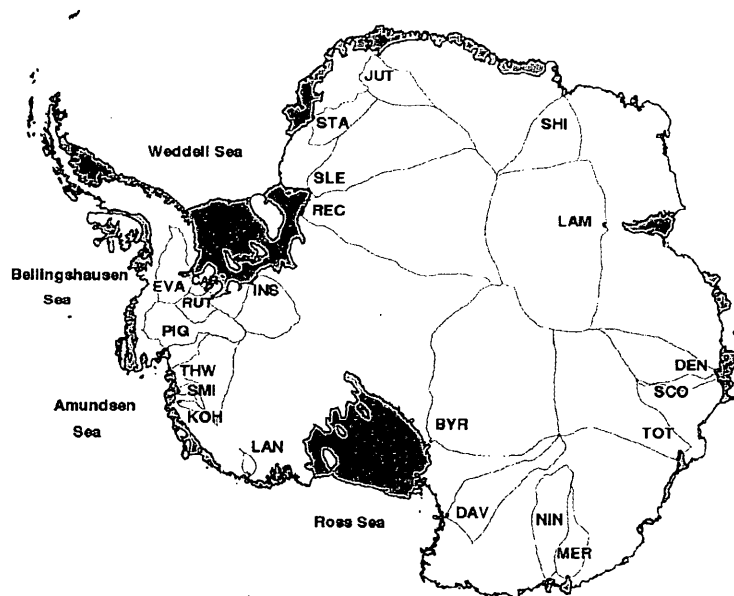
Eric Rignot

tel, 818-354-1640; fax, 818-393-3077; email, eric@adelle.jpl.nasa.gov

NASA Earth Science Enterprise Strategic Plan Question

What changes are occurring in the mass of the Earth's ice cover?

We surveyed a large number of Antarctic glaciers using ERS InSAR data to determine their state of mass balance by comparing the ice discharge at the grounding line with snow accumulation in the interior. The results suggest no gross imbalance between discharge and accumulation in East Antarctica. Prior estimates of large positive mass budget for the Lambert/Amery system were caused by a mis-positioning of the grounding line. In West Antarctica, the glaciers draining into the Ronne Ice Shelf are close to a state of mass balance, but those draining into the Amundsen Sea are significantly out of balance. The two largest glaciers, Pine Island and Thwaites Glaciers, are thinning rapidly, retreating and losing mass to the ocean. A significant amount of mass loss is also detected along other smaller glaciers draining into the Getz ice shelf. Our analysis of ice-shelf basal melting combined with ocean data indicates a high sensitivity to thermal forcing from the ocean. The documented demise of these ice shelves could be due to the ocean warming recently reported for this region.



Location map of the 22 Antarctic glaciers surveyed with ERS and RSAT InSAR. The ADD ice front and grounding line positions are black, drainage basins are green, the InSAR grounding-line flux gates are red and ice shelves are blue.

Study of Coastal Ocean Dynamics for Predicting Coastal Environmental Changes

Y. Tony Song

tel, 818-393-4876; fax, 818-393-6720; email, song@pacific.jpl.nasa.gov

NASA Earth Science Enterprise Strategic Plan Question

What are the consequences of climate and sea level changes and increased human activities on coastal regions?

The coastal ocean is a region extending from the surf zone to the edge of the continental rise, an area generally ranging from 100 to 1000 kilometers wide and including large inland water bodies, and serves as an interface between land-derived materials and impacts from the open ocean. It is characterized by high temporal and spatial variability, high biological productivity, and intense air-sea-land interaction (e.g., Figure 1). Human activity profoundly affects the coastal ocean, and coastal waters, in turn, influence the lives of the vast and increasing populations that live nearby.

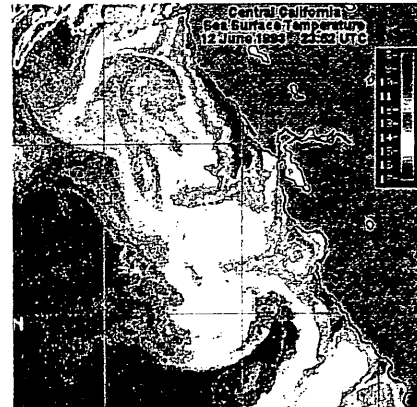


Figure 1. Satellite image of SST shows multiple upwelling centers (Courtesy E. Armstrong).

My research strategy is to use high-resolution, coupled physical-biological coastal ocean models, nested in large-scale ocean models, to assess both long-term and short-term impacts of natural changes on coastal environments. For example, using a high-resolution coastal model, Song et al. (2000) determined five offshore transport jets along the northern California region (Figure 2) and each carries 5 to 15 Sv of coastal water offshore. It was found that the topographic variability plays an important role in the formation of the coastal upwelling centers and jets (Song et al., 2001). Such kinds of jets have important implications for estimating coastal fluxes in global biogeochemical studies. My study will focus on the following objectives:

- (1) Assess the impact of the time-space variability of local and remote forcings on the formation of coastal upwelling and frontal variability.
- (2) Quantify coastal ocean response to extreme wind events, such as tropical storms and hurricanes.
- (3) Determine the controlling factors of the cross-shore exchange and the subsequent impacts of that exchange on biogeochemical cycling.

This study will provide the scientific base that is required for comprehensive understanding of coastal environments and will help set criteria for improving future NASA missions to accommodate coastal studies. The synergistic applications of satellite measurements to the multi-scale coastal models are prototypes for future improvements in coastal hazard prediction and global biogeochemical modeling with embedded coastal oceans.

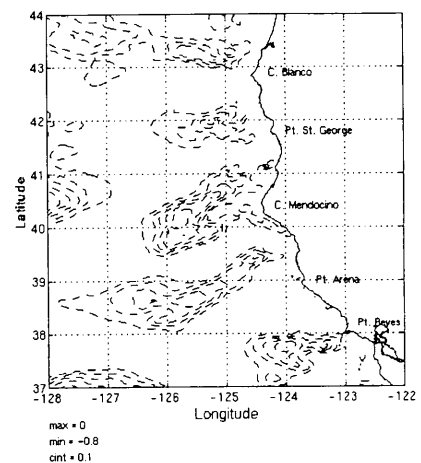


Figure 2. Model results showing multiple cross-shore transport jets off the US West coast (Song et al., 2000).

Synergistic Use of TRMM and SeaWinds Data

Michael W. Spencer

tel, 818-354-1175; fax, 818-593-5184; email, michael.w.spencer@jpl.nasa.gov

NASA Earth Science Enterprise Strategic Plan Question

How can weather forecast duration and reliability be improved by new space-based observations, data assimilation, and modeling?

A major limitation to using SeaWinds scatterometer measurements to infer surface winds within storms is the presence of rain. The backscatter and attenuation produced by rain is observed to produce significant errors in Ku-Band scatterometer wind retrievals. Because the signal from the ocean surface and the corrupting signal from the rain are difficult to separate in the scatterometer data, it is desirable to have independent measurements of the rain only. Such comparison data is provided by the Tropical Rainfall Mapping Mission (TRMM) precipitation radar (PR). In areas where TRMM data is collocated with SeaWinds data, the complete surface/atmosphere scattering phenomenology can be studied. The purpose of this research is to use SeaWinds and TRMM data synergistically to better characterize the effects of rain on scatterometer measurements, and to investigate techniques whereby rain contamination may be removed to produce better spaceborne wind estimates within storms. The SeaWinds measurements also provide improved background wind fields leading to more accurate TRMM rain estimates.

In an effort to better understand the effects of rain on the scatterometer measurements we use a mathematical model for the observed SeaWinds sigma-0 values. In the model, the observed SeaWinds sigma-0 is a linear combination of wind-induced and rain-induced surface backscatter, multiplied by the two-way attenuation, plus the backscattering contribution from the falling rain. Using a collocated database of TRMM PR and SeaWinds data where measurements from the two sensors overlap within 10 minutes of each other, we average the PR integrated rain sigma-0 values, path-integrated attenuation, and rain rates over the collocated SeaWinds footprint, creating what are, in effect, SeaWinds observations of each of these parameters. Solving for the rain-induced surface sigma-0 and assuming a power law dependence of surface sigma-0 on rain rate, a relationship between rain-induced surface sigma-0 and the rain rate is derived for SeaWinds incidence angles. Since both the two-way attenuation and rain reflectivity are related to the rain rate, it is possible to estimate not only the wind-induced sigma-0, but also the rain rate using only the scatterometer data.

This research is performed in collaboration with David G. Long of Brigham Young University.

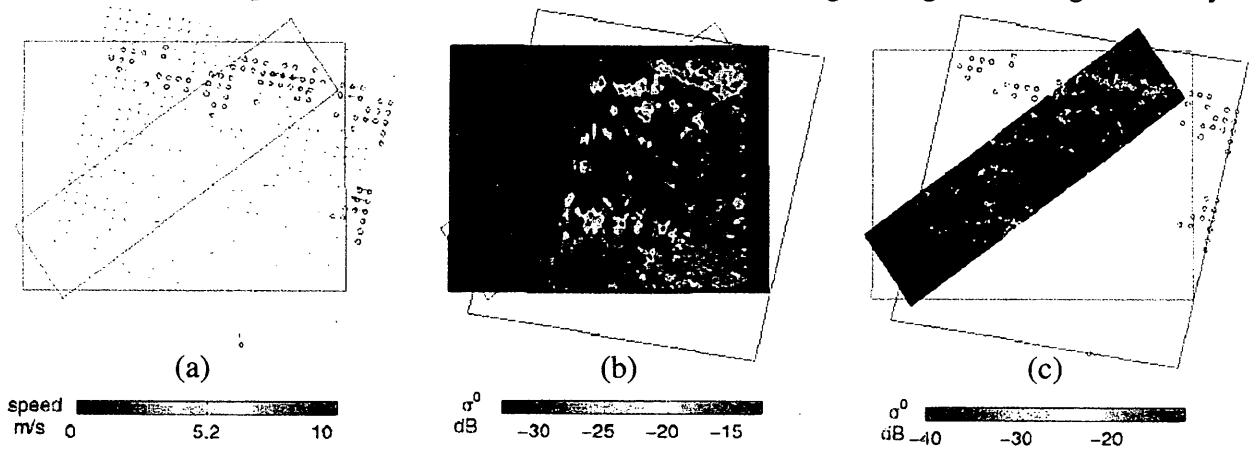


Image (a) shows SeaWinds wind vectors and rain flags (circles); (b) shows scatterometer sigma-0 values obtained over raining region; and (c) shows effective scatterometer sigma-0 values derived from TRMM PR data.

Vertical Distribution of Aerosol Backscatter over the Pacific Ocean

David M. Tratt

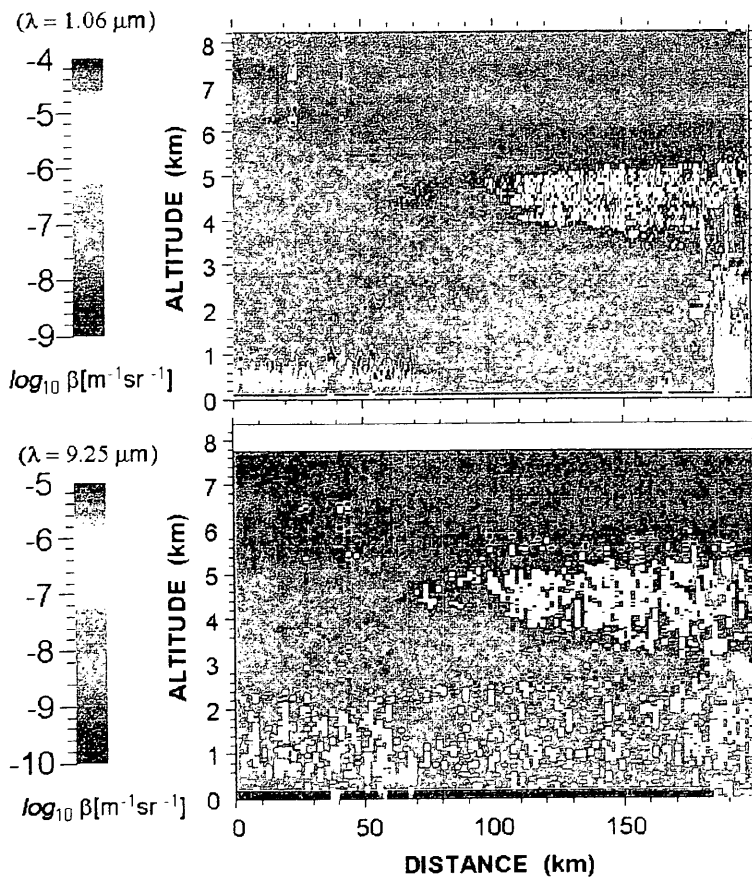
tel, 818-354-2750; fax, 818-393-6984; email, david.tratt@jpl.nasa.gov

NASA Earth Science Enterprise Strategic Plan Question

What trends in atmospheric constituents and solar radiation are driving global climate?

Knowledge of the optical properties of the atmospheric aerosols is critical to the analysis of their direct effect on the radiation budget and hence the Earth's climate. Because of the spatial variability of the aerosol particle concentration and composition due to their relatively short lifetime and the diversity of sources, regional effects can be much different from global average forcing calculations. The GLOBE (Global Backscatter Experiment) flight series conducted in Nov/Dec 1989 and in May/June 1990 covered a wide latitude range over the Pacific Ocean using the NASA DC-8 research aircraft whose instrument complement included two pulsed backscatter lidars for high-resolution vertical profiling of the aerosol scattering. The lidar fielded by JPL operated at 9.25 μm while the second system, provided by NASA GSFC, operated at 1064, 532, and 1540 nm.

An example of the high correlation seen in a highly-structured aerosol environment is shown in the accompanying figure. These observations were acquired during a direct flight from Tokyo to



Honolulu, ~1800 km from Tokyo, on June 4, 1990. The layered structure of the aerosol in the free troposphere is observed at both lidar wavelengths, as well as the broken cloud cover at the top of the convective boundary layer in the first 70 km of the plot and the altocumulus structures at 180-200 km (which have sufficient optical depth to cause loss of signal from beneath them). These aerosol layers were observed to be primarily Asian dust, based on measurements of the aerosol at flight altitude using *in situ* instruments along with trajectory analyses.

Further results from the GLOBE flight series relating to these issues are in press. The 1.064- μm micron data presented here were made available by NASA GSFC.

2-cm GPS Altimetry Over Crater Lake

Robert Treuhaft

tel, 818-354-6216; fax, 818-393-5115; email, robert.treuhaft@jpl.nasa.gov

NASA Earth Science Enterprise Strategic Plan Question

What are the consequences of climate and sea level changes and increased human activities on coastal regions?

The highest precision Global Positioning System (GPS) altimetry to date was performed over Crater Lake in October 1999 and reported with a cover photo in *Geophysical Research Letters* in December 2001. This experiment probed fundamental parts of the air- and spaceborne GPS error budget for ocean altimetry, and it was also the first step toward altimetry of the coastal oceans with fixed receivers. Airborne, spaceborne, and coastal GPS altimetry will monitor ocean eddies, the understanding of which is vital to environmental studies. These whirlpool-like features serve as nutrient-rich environments which foster and transport juvenile plants and fish. Oceanographers also believe that eddies can affect the dispersal of pollution.

Using a GPS antenna and receiver on Cloudcap Lookout at an altitude of about 480 meters above the lake surface, researchers at JPL measured the phase of the GPS signal. This phase depends on the difference between the arrival time of the signal traveling directly from the GPS satellite and that from the lake-reflected path. A simple physical model was used to estimate the altitude of the receiver from the GPS phase. These altitudes, shown in Figure 1 below as a function of time, exhibited a precision of about 2 cm in 1 second. Thermal noise from the receiver and tropospheric fluctuations were responsible for the scatter in the figure. Coauthors are Stephen Lowe, Cinzia Zuffada, and Yi Chao.

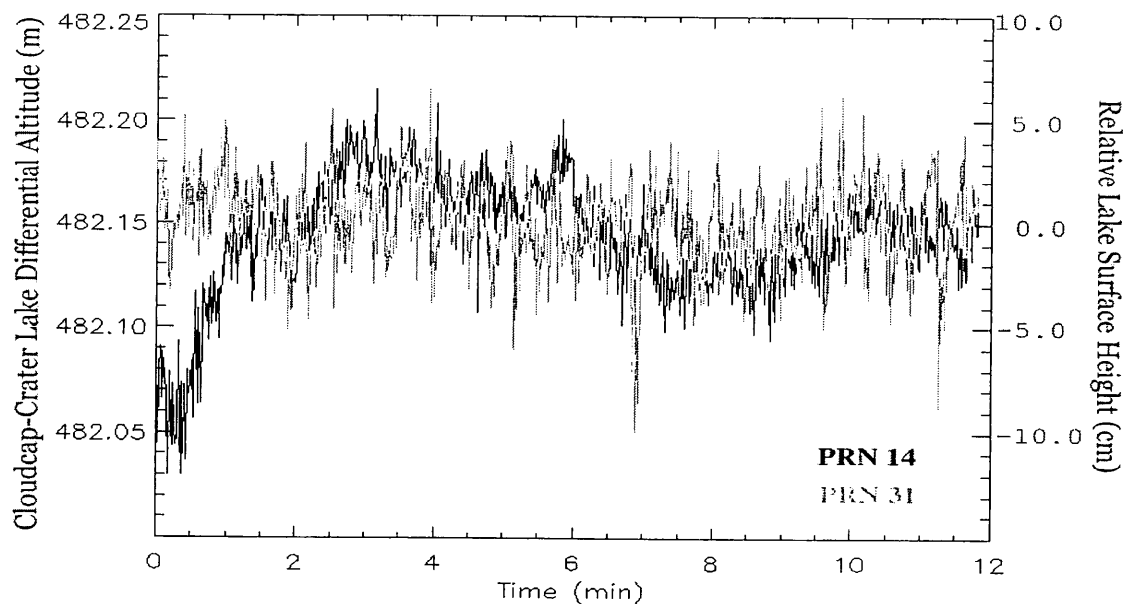


Figure 1: The altitude of the GPS receiver at the Cloudcap Lookout over Crater Lake, as a function of time, for two satellites. The black line is from PRN 14 data, and gray line is from PRN 31.

CloudSat Mission Observations Will Improve Understanding of Cloud-Climate Interactions

Deborah Vane

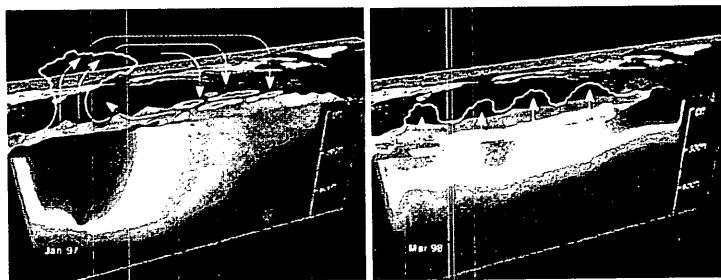
tel, 818-354-3708; fax, 818-393-9899; email, dvane@jpl.nasa.gov

NASA Earth Science Enterprise Strategic Plan Question

What are the effects of clouds and surface hydrologic processes on Earth's climate?

Clouds exert an enormous influence on our weather and climate through their effect on the Earth's solar and thermal radiation budgets. By modulating the pole-to-equator variations of both the solar insolation reaching the surface and the radiation emitted to space, and by altering the distribution of heating within the atmosphere, clouds fundamentally influence the global circulation of the atmosphere and of the oceans. Understanding cloud-climate interactions is fundamental to the study of climate variability and climate change and is the focus of the CloudSat mission under development at JPL, to be launched in 2004.

Climate models must portray clouds realistically if they are to provide accurate predictions of the atmospheric hydrologic cycle. Cess et al. (2001) observed substantial differences in cloud heights across the tropical Pacific Ocean during the 1997-1998 El Niño. The 1998 El Niño was so strong that it evenly distributed warm water across all of the Pacific Ocean, and the lack of a temperature difference between the Eastern and Western Pacific collapsed the atmospheric circulation known as the Walker cell. The normal Walker cell consists of air rising over Indonesia in the western Pacific Ocean and sinking off the west coast of South America. Trade winds blowing east to west fuel this circulation and drag ocean surface waters with them. During El Niño years, as the trade winds subside, warm waters in the western and central tropical Pacific Ocean spread east into colder waters, lessening the difference in east and west sea surface temperatures. The 1998 El Niño was so strong, there was no temperature gradient. The collapse of the Walker cell during the 1998 event allowed for rising air over the eastern tropical Pacific Ocean, normally an area of subsidence, and the collapse caused lower clouds in the west and higher clouds in the eastern Pacific during the 1998 El Niño (figure on right) as compared to normal years (figure on left).



(Images courtesy of NASA SVS).

The CloudSat 94-GHz cloud profiling radar will provide the first global observations of the vertical structure of clouds that will further improve the representation of cloud-climate interactions.

Polarimetric Radar Remote Sensing of Ocean Wind

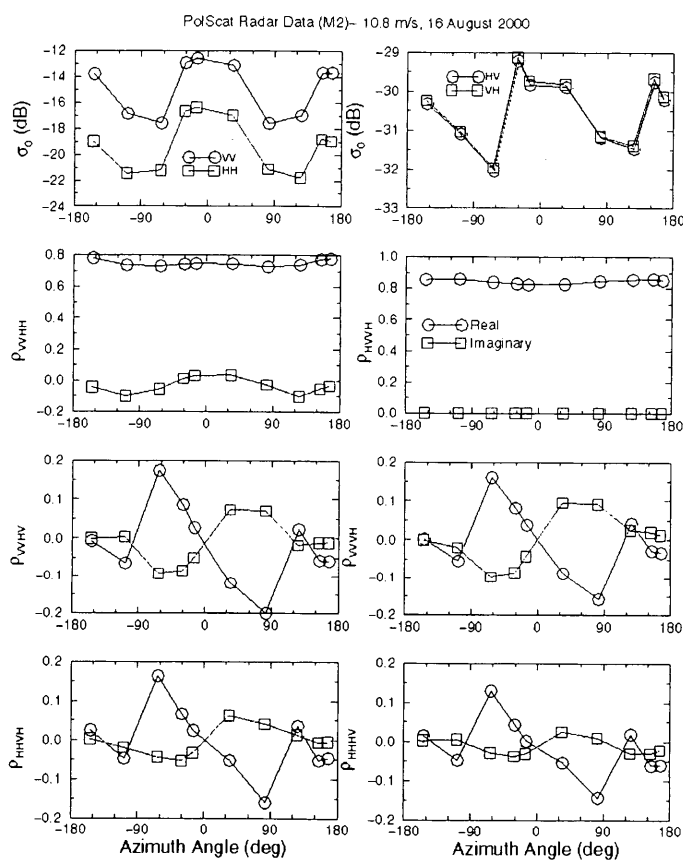
Simon H. Yueh

tel, 818-354-3012; fax, 818-393-3077; email: simon.yueh@jpl.nasa.gov

NASA Earth Science Enterprise Strategic Plan Question

How is the global ocean circulation varying on interannual, decadal, and longer time scales?

The objective of this research is to develop the polarimetric radar technique for global ocean wind measurements with unique wind direction determination capability. This will overcome a key remaining deficiency of present spacecraft scatterometers. The Jet Propulsion Laboratory polarimetric scatterometer (POLSCAT) was built and deployed on the National Center for Atmospheric Research (NCAR) C-130 aircraft for proof-of-concept flights in August 2000. Several flights over the Monterey Bay Aquarium Research Institute buoys were completed.



The experimental data illustrated above show that the backscattering coefficients, σ_{HH} , σ_{VV} , σ_{HV} , and ρ_{VVHH} are symmetric with respect to the wind direction, while the correlation between co- and cross-polarized scattering signals, including ρ_{VVHV} , ρ_{VVHH} , ρ_{HHHV} , and ρ_{HHHV} , has an odd symmetry. The complementary symmetry properties in the data demonstrate the polarimetric radar concept for ocean wind measurements from space.

Effect of Wind Stress Parameterization on an Ocean Model and GRACE Ocean Validation

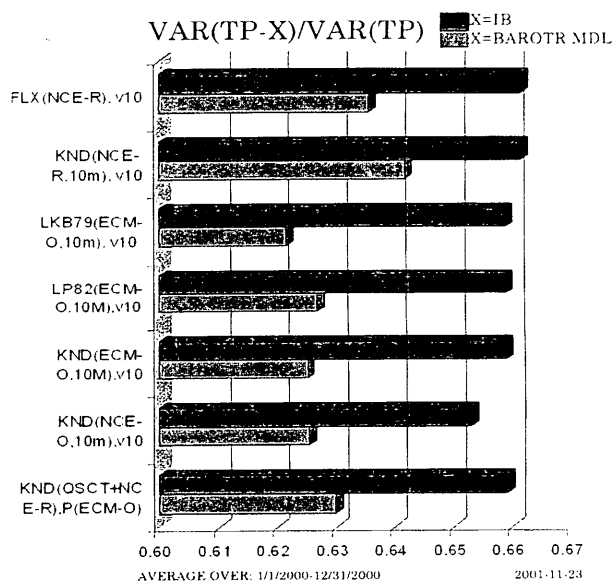
Victor Zlotnicki

tel, 818-354-5519; fax, 818-393-6720; email, vz@pacific.jpl.nasa.gov

NASA Earth Science Enterprise Strategic Plan Question

How is the global ocean circulation varying on interannual, decadal, and longer time scales?

Using a barotropic ocean model, Drs. Ahmed Ali and Victor Zlotnicki assessed the effect of different atmospheric model sources and wind stress parameterizations on the ocean model's ability to fit short-period energy in Topex/Poseidon altimetry for the year 2000. We tested wind and pressure data from the European Center for Medium Range Weather Forecast (ECMWF) and from the National Center for Environmental Prediction (NCEP), two well-known neutral-stability algorithms (Large and Pond, 1982, and Kondo, 1975), as well as one algorithm that simultaneously solves for the fluxes of heat, momentum, and water (Liu et al., 1979). We find (figure to the right) that the operational NCEP model in 2000 performs substantially better than the NCEP reanalysis model, not surprising since the NCEP reanalysis is carried out with a 1994 version of the atmospheric model. For a given atmospheric model's 10 m wind, we find that the Liu et al. algorithm performs substantially better, because over most the oceans, most of the time, the boundary layer is unstable.



In separate work, in collaboration with Dr. Steven Jayne (Woods Hole Oceanographic Institution), we assessed the criteria to deploy an ocean validation experiment for GRACE. This U.S.-German mission will measure the gravity field for 5 years, which can be converted to monthly estimates of time changes in 1000-km averaged ocean-bottom pressure, with an



BOTT PRESS, MONTH-AVE, SHORT WAVEL: STDDEV(BP-10DegAve(BP)), mbar. ECCO CTL 2000-06

expected accuracy of 0.1 mbar. Our criteria to validate such claims include the accuracy of bottom pressure recorders on monthly and interannual scales, their ability to stay in the water for 4 or more years, the spatial variability of bottom pressure on scales shorter than 1000 km (figure to the left), the contamination of GRACE data from time-varying land hydrology and from short-period ocean signals, as well as logistic considerations which impinge on the total price tag of such a campaign. We concluded that an experiment in the N.W. Atlantic at 16°N with about 10 bottom pressure sensors provides an excellent opportunity for such a validation.

GPS Altimetry

Cinzia Zuffada

tel, 818-354-0033; fax, 818-393-4965; email, cinzia@cobra.jpl.nasa.gov

NASA Earth Science Enterprise Strategic Plan Question

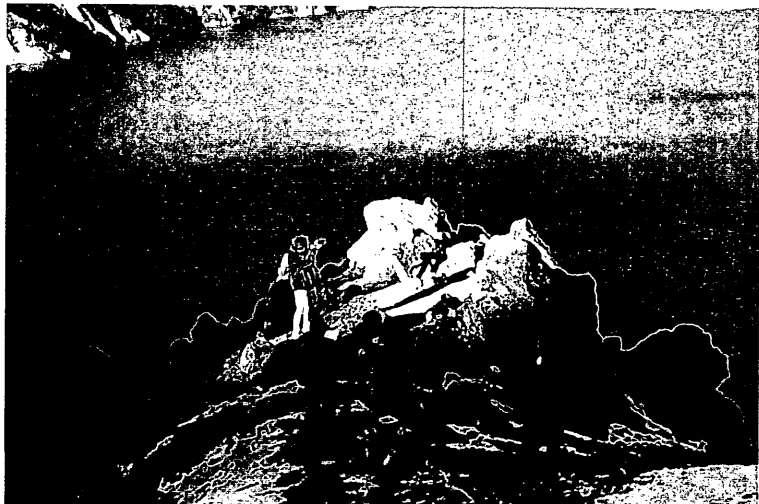
How is the global ocean circulation varying on interannual, decadal, and longer time scales?

Ocean eddies, analogous to atmospheric storms, play an important role in the transport of momentum, heat, salt, nutrients, and other chemical properties of the ocean. Ocean eddies have a typical spatial scale on the order of 100 km and a temporal scale from days to weeks. The sea level is usually 10 cm or more. At present, quantifying the role of mesoscale eddies in the ocean circulation and therefore climate variability cannot be done simply, because their spatio-temporal structures are not resolved by the conventional remote-sensing techniques.

We have demonstrated the possibility of using the Global Positioning System (GPS) signals scattered off the ocean and sensed by an air- or spaceborne receiver in a bistatic radar geometry as a means of doing ocean altimetry. When considering the constellation of 24 GPS transmitters and one such receiver, a multistatic system is obtained capable of intercepting bounces from several areas of the ocean simultaneously, and hence map the entire Earth surface in just 1 day. Such dense coverage can be translated into a higher temporal and spatial resolution than TOPEX/Poseidon or the proposed wide swath altimeter, thereby providing the ability to recover certain ocean topography features or processes that are precluded with traditional altimeters.

To assess the feasibility of this new type of measurement, we need to understand its accuracy as a function of the sea-state, the many relevant system parameters, and the observational geometry. We performed a simple altimetric experiment, where the receiver is at a fixed location over a lake, as shown in the figure. A lake reduces the surface roughness, a condition likely to be reproduced in the ocean at low elevation angles. This set up allows us to understand the limiting systematic measurement errors associated with the technique. The experiment yields 2-cm precision altimetry in 1 sec using two satellites.

The next steps involve obtaining the measurement precision over the ocean, using a receiver on a moving platform. We performed a flight campaign off the coast of Southern California, along the TOPEX track passing through Harvest oil platform. The precision obtained is 5 cm with 5 km resolution in 1 sec. This is suitable for measurements of mesoscale processes. In the future we are planning more work to understand the measurement accuracy.





Appendix A.

2000-2001 Publications



Appendix A.

2000 – 2001 Publications

- Aponte, N., S. A. Gonzalez, M. C. Kelley, C. A. Tepley, **X. Pi**, and B. A. Iijima. 2000. Advection of the equatorial anomaly over Arecibo by small-storm related disturbance dynamo electric fields. *Geophys. Res. Lett.* 27:2833-2836.
- Bamber, J. L., D. G. Vaughan, and **I. Joughin**. 2000. Widespread complex flow in the interior of the Antarctic ice sheet. *Science* 287:1248-1250.
- Bamber, J. L., R. J. Hardy, and **I. Joughin**. 2000. An analysis of balance velocities over the Greenland Ice Sheet and comparison with synthetic aperture radar interferometry. *J. Glacio.* 46:67-74.
- Barber, R. T., J. Marra, R. C. Bidigare, L. A. Codispoti, **D. Halpern**, Z. Johnson, M. Latasa, R. Goericke, and S. L. Smith. 2001. Primary production and its regulation in the Arabian Sea during 1995. *Deep-Sea Res. II* 48:1127-1172.
- Bindschadler, R., and **E. Rignot**. 2001. "Crack!" in the polar night. *Eos* 82:497-505.
- Blanco, J. L., A. C. Thomas, **M.-E. Carr**, and P. T. Strub. 2001. Seasonal climatology of hydrographic conditions in the upwelling region off northern Chile. *J. Geophys. Res.* 106:11451-11467.
- Brown, R. G., and **L.-L. Fu**. 2000. An examination of the spring 1997 mid-latitude east Pacific sea surface temperature anomaly. *Atmosphere-Ocean* 38:577-599.
- Cailliau, D., and **V. Zlotnicki**. 2000. Precipitation detection by the TOPEX/Poseidon dual-frequency radar altimeter, TOPEX microwave radiometer, special sensor microwave/imager and climatological ship reports. *IEEE Trans. Geosci. Remote Sensing* 38:205-213.
- Carr, M.-E.**, and K. Broad. 2000. Satellites, society, and the Peruvian fisheries during the 1997-1998 El Niño. In *Satellites, Oceanography and Society*, ed. **D. Halpern**, 171-190. Amsterdam: Elsevier Science Publishers.
- Carr, M.-E.**, and H. T. Rossby. 2001. Pathways of the North Atlantic Current from surface drifters and subsurface floats. *J. Geophys. Res.* 106:445-4419
- Cassou, C., and **C. Perigaud**. 2000. ENSO simulated with intermediate coupled models and evaluated with observations over 1970-1996. Part II: role of the off-equatorial ocean and meridional winds. *J. Climate* 13:1635-1663.
- Chang, J., and **Y. Chao**. 2000. A comparison between the World Ocean Atlas and hydrobase climatology. *Geophys. Res. Lett.* 27:1191-1194.

- Chao, Y.**, and M. S. Lozier. 2001. Evaluation of North Atlantic property field simulations at $1/6^\circ$. *J. Phys. Oceanogr.* 31:3200-3213.
- Chao, Y.**, M. Ghil, and J. C. McWilliams. 2000. Pacific interdecadal variability in this century's sea surface temperature. *Geophys. Res. Lett.* 27:2261-2264.
- Chelton, D. B., J. Ries, **B. Haines**, **L.-L. Fu**, and P. Callahan. 2001. Satellite altimetry. In *Satellite Altimetry and Earth Sciences: A Handbook for Techniques and Applications*, ed. **L.-L. Fu** and A. Cazenave, 1-131. San Diego: Academic Press.
- Chu, P. C., C. Fan, and **W. T. Liu**. 2000. Determination of vertical thermal structure from sea surface temperature. *J. Atmos. Ocean. Tech.* 17:971-979.
- Chu, P., J. M. Veneziano, C. Fan, M. J. Carron, and **W. T. Liu**. 2000. Response of the South China Sea to Tropical Cyclone Ernie, 1996. *J. Geophys. Res.* 105:13991-14009.
- deViron, O., **S. L. Marcus**, and **J. O. Dickey**. 2001. Atmospheric torques during the winter of 1989: impact of ENSO and NAO positive phases. *Geophys. Res. Lett.* 28:1985-1988.
- deViron, O., **S. L. Marcus**, and **J. O. Dickey**. 2001. Diurnal angular momentum budget of the atmosphere and its consequences for the Earth's nutation, *J. Geophys. Res.* 106:26747.
- Dickey, J. O.** 2001. Time variable gravity: an emerging frontier in interdisciplinary geodesy gravity. In *Proceedings of Gravity, Geoid, and Geodynamics 2001*, 1-7. New York: Springer-Verlag.
- DiGiacomo, P. M., and **B. Holt**. 2001. Satellite observations of small coastal ocean eddies in the Southern California Bight. *J. Geophys. Res.* 106:22521-22544.
- Diner, D. J., W. A. Abdou, J. E. Conel, K. A. Crean, B. J. Gaitley, M. Helmlinger, **R. A. Kahn**, J. V. Martonchik, and S. H. Pilorz. 2001. MISR aerosol retrievals over southern Africa during the SAFARI-2000 dry season campaign. *Geophys. Res. Lett.* 28:3127-3130.
- Durden, S. L.**, **E. Im**, **F. K. Li**, R. Girard, and K. Pak. 2001. Surface clutter due to antenna sidelobes for spaceborne atmospheric radar. *IEEE Trans. Geosci. Remote Sensing* 39:1916-1921.
- Dushaw, B., G. Bold, C.-S. Chiu, J. Colosi, B. Cornuelle, Y. Desaubies, M. Dzieciuch, A. Forbes, F. Gaillard, A. Gavrilov, J. Gould, B. Howe, M. Lawrence, J. Lynch, **D. Menemenlis**, J. Mercer, P. Mikhalevsky, W. Munk, I. Nakano, F. Schott, U. Send, R. Spindel, T. Terre, P. Worcester, and C. Wunsch. 2001. Observing the ocean in the 2000s: a strategy for the role of acoustic tomography in ocean climate observation. In *Observing the Oceans in the 21st Century*, ed. C. J. Koblynski and N. R. Smith, 391-418. Melbourne: Bureau of Meteorology.
- Fahnestock, M., W. Abdalati, **I. Joughin**, J. Brozena, and P. Gogineni. 2001. High geothermal heat flow, basal melt, and the origin of rapid ice flow in central Greenland. *Science.* 294:2338-2342.

- Fahnestock, M. A., **I. Joughin**, T. A. Scambos, **R. Kwok**, W. B. Krabill, and S. Gogineni. 2001. Ice stream related patterns of ice flow in the interior of northeast Greenland. *J. Geophys. Res.* 106:34035-34046.
- Fahnestock, M. A., T. A. Scambos, C. A. Shuman, R. J. Arthern, D. P. Winebrenner, and **R. Kwok**. 2000. Snow megadune fields on the East Antarctic Plateau: extreme atmosphere-ice interaction. *Geophys. Res. Lett.* 27:3719-3722.
- Fu, L.-L.** 2001. Ocean circulation and variability from satellite altimetry. In *Ocean Circulation and Climate*, ed. J. Church, G. Siedler, and J. Gould, 141-172. San Diego: Academic Press.
- Fu, L.-L.**, and D. B. Chelton. 2001. Large-scale ocean circulation. In *Satellite Altimetry and Earth Sciences: A Handbook for Techniques and Applications*, ed. **L.-L. Fu** and A. Cazenave, 131-169. San Diego: Academic Press.
- Fu, L.-L.**, B. Cheng, and B. Qiu. 2001. 25-Day period large-scale oscillations in the Argentine Basin revealed by the TOPEX/Poseidon altimeter. *J. Phys. Oceanogr.* 31:506-517.
- Fukumori, I.** 2000. Data assimilation by models. In *Satellite Altimetry and Earth Sciences: A Handbook of Techniques and Applications*, ed. **L.-L. Fu** and A. Cazenave, 237-265. San Diego: Academic Press.
- Gangopadhyay, A., and **Y. Chao**. 2000. Sensitivity of the Gulf Stream path to the cyclonic wind stress curl. *Global Atmosphere Ocean System* 7:151-178.
- Garcia, F. J., M. C. Kelley, J. J. Makela, P. J. Sultan, **X. Pi**, and S. Musman. 2000. Mesoscale structure of the midlatitude ionosphere during high geomagnetic activity: airglow and GPS observations. *J. Geophys. Res.* 105:18417-18427.
- Garcia-Gorriz, E., and **M.-E. Carr**. 2001. Physical control of phytoplankton distributions in the Alboran Sea: a numerical and satellite approach. *J. Geophys. Res.* 106:16795-16805.
- Gross, R. S.** 2000. The excitation of the Chandler wobble. *Geophys. Res. Lett.* 27:2329-2332.
- Gross, R. S.** 2001. Gravity, oceanic angular momentum, and the Earth's rotation. In *Gravity, Geoid, and Geodynamics 2000*, ed. M. G. Sideris, 153-158. New York: Springer-Verlag.
- Hajj, G. A.**, L. C. Lee, **X. Pi**, L. J. Romans, W. S. Schreiner, P. R. Straus, and C. Wang. 2000. COSMIC GPS ionospheric sensing and space weather. *Terr. Atmos. Ocean. Sci.* 11:235-272.
- Halpern, D.**, and C.-W. Hung. 2001. Satellite observations of the southeast Pacific convergence zone during 1993-1998. *J. Geophys. Res.* 106:28107-28112.
- Halpern, D.**, and P. M. Woiceshyn. 2001. Somali Jet in the Arabian Sea, El Niño, and India rainfall. *J. Climate* 14:434-441.

- Harris, I. L., A. J. Mannucci, B. A. Iijima, U. J. Lindqwister, D. Muna, **X. Pi**, and B. D. Wilson. 2001. Ionospheric specification algorithms for precise GPS-based aircraft navigation. *Radio Sci.* 36:287-298.
- Hashizume, H., S.-P. Xie, **W. T. Liu**, and K. Takeuchi. 2001. Local and remote atmospheric response to tropical instability waves: a global view from space. *J. Geophys. Res.* 106:10173-10185.
- Hirose, N., **I. Fukumori**, and R. Ponte. 2001. A non-isostatic global sea level response to barometric pressure near 5-days. *Geophys. Res. Lett.* 28:2441-2444.
- Hirose, N., **I. Fukumori**, **V. Zlotnicki**, and R. Ponte. 2001. High-frequency barotropic ocean response to atmospheric disturbances: sensitivity to forcing, topography, and friction. *J. Geophys. Res.* 106:30987-30995.
- Holt, B.**, and J. Hilland. 2000. Rapid-repeat SAR imaging of the ocean surface: are daily observations possible? *Johns Hopkins APL Technical Digest* 21:162-169.
- Holt, B.**, and S. Martin. 2001. The effect of a storm on the 1992 summer sea ice cover of the Beaufort, Chukchi, and East Siberian Seas. *J. Geophys. Res.* 106:1017-1032.
- Hulbe, C. L., **I. Joughin**, D. Morse, and B. Bindschadler. 2000. Tributaries to West Antarctic ice streams: characteristics deduced from numerical modeling of ice flow. *Ann. Glacio.* 31:184-190.
- Husar, R. B., **D. M. Tratt**, B. A. Schichtel, S. R. Falke, F. Li, D. Jaffe, S. Gassó, T. Gill, N. S. Laulainen, F. Lu, M. C. Reheis, Y. Chun, D. Westphal, B. N. Holben, C. Geymard, I. McKendry, N. Kuring, G. C. Feldman, C. McClain, R. J. Frouin, J. Merrill, D. DuBois, F. Vignola, T. Murayama, S. Nickovic, W. E. Wilson, K. Sassen, N. Sugimoto, and W. C. Malm. 2001. Asian dust events of April 1998. *J. Geophys. Res.* 106:18317-18330.
- Ivins, E. R.**, C. A. Raymond, and T. S. James. 2000. The influence of 5000 year-old and younger glacial mass variability on present-day crustal rebound in the Antarctic peninsula. *Earth, Planets and Space* 52:1023-1029.
- Ivins, E. R.**, X. Wu, C. A. Raymond, C. F. Yoder, and T. S. James. 2001. Temporal geoid of a rebounding Antarctica and potential measurement by the GRACE and GOCE satellites. In *Gravity, Geoid and Geodynamics 2000*, ed. M. Sideras, 361-366. New York: Springer-Verlag.
- Joughin, I. R.**, M. Fahnestock, and J. Bamber. 2000. Ice flow in the Northeast Greenland Ice Stream. *Ann. Glacio.* 31:141-146.
- Joughin, I.**, M. Fahnestock, D. MacAyeal, J. Bamber, and P. Gogineni. 2001. Observation and analysis of ice flow in the largest Greenland ice stream. *J. Geophys. Res.* 106:34021-34034.
- Kahn, R.**, P. Banerjee, and D. McDonald. 2001. The sensitivity of multiangle imaging to natural mixtures of aerosols over ocean. *J. Geophys. Res.* 106:18219-18238.

- Kahn, R.**, P. Banerjee, D. McDonald, and J. Martonchik. 2001. Aerosol properties derived from aircraft multi-angle imaging over Monterey Bay. *J. Geophys. Res.* 106:11977-11995.
- Katsaros, K. B., E. B. Forde, P. Chang, and **W. T. Liu**. 2001. QuikSCAT facilitates early identification of tropical depressions in 1999 hurricane season. *Geophys. Res. Lett.* 28:1043-1046.
- Keihm S., **V. Zlotnicki**, and C. Ruff. 2000. TOPEX microwave radiometer performance evaluation, 1992-1998. *IEEE Trans. Geosci. Remote Sens.* 38:1379-1386.
- Kinne, S., B. Holben, T. Eck, A. Smirnov, O. Dubovik, I. Slutsker, D. Tanre, G. Zibozdi, U. Lohmann, S. Ghan, R. Easter, M. Chin, P. Ginoux, T. Takemura, I. Tegen, D. Koch, **R. Kahn**, E. Vermote, L. Stowe, O. Torres, M. Mishchenko, I. Geogdzhayev, and A. Hiragushi. 2001. How well do aerosol retrievals from satellites and representation in global circulation models match ground-based AERONET aerosol statistics? In *Remote Sensing and Climate Modeling: Synergies and Limitations*, ed. M. Beniston and M. M. Verstraete, 103-158. Dordrecht: Kluwer Academic Publishers.
- Kursinski, E. R.**, and **G. A. Hajj**. 2001. A comparison of water vapor derived from GPS occultations and global weather analyses. *J. Geophys. Res.* 106:1113-1138.
- Kursinski, E. R.**, **G. A. Hajj**, S. S. Leroy, and B. Herman. 2000. The GPS radio occultation technique. *Terr. Atmos. Oceanic Sci.* 11:53-114.
- Kwok, R.** 2000. Recent changes of the Arctic Ocean sea ice motion associated with the North Atlantic Oscillation. *Geophys. Res. Lett.* 27:775-778.
- Kwok, R.** 2001. Deformation of the Arctic Ocean sea ice cover: November 1996 through April 1997. In *Scaling Laws in Ice Mechanics and Dynamics*, ed. J. Dempsey and H. H. Shen, 315-323. Dordrecht: Kluwer Academic.
- Kwok, R.**, M. Seigert, and **F. D. Carsey**. 2001. Ice motion over Lake Vostok. *J. Glacio.* 46:689-694.
- Lee, T.**, J.-P. Boulanger, A. Foo, **L.-L. Fu**, and R. Giering. 2000. Data assimilation by an intermediate coupled ocean-atmosphere model: application to the 1997-1998 El Niño. *J. Geophys. Res.* 105:26063-26087.
- Legresy, B., **E. Rignot**, and I. E. Tabacco. 2000. Constraining ice dynamics at Dome C, Antarctica, using remotely sensed measurements. *Geophys. Res. Lett.* 27:3493-3496.
- Li, L., S. M. Sekelsky, S. C. Reising, C. T. Swift, **S. L. Durden**, G. A. Sadowy, S. J. Dinardo, **F. K. Li**, A. Huffman, G. Stephens, D. M. Babb, and H. W. Rosenberger. 2001. Retrieval of atmospheric attenuation using combined ground-based and airborne 95 GHz cloud radar measurements. *J. Atmos. Oceanic Technol.* 18:1345-1353.

- Li, X., Q. Zheng, W. G. Pichel, X.-H. Yan, **W. T. Liu**, and P. Clemente-Colon. 2001. Analysis of coastal lee waves along the coast of Texas observed in AVHRR image. *J. Geophys. Res.* 106:7017-7025.
- Li, X., **Y. Chao**, J. C. McWilliams, and **L.-L. Fu**. 2001. A comparison of two vertical mixing schemes in a Pacific Ocean General Circulation Model. *J. Climate* 14:1377-1398.
- Liu, W. T.** 2001. Wind over troubled water. *Backscatter* 12, no. 2:10-14.
- Liu, W. T.**, and K. B. Katsaros. 2001. Air-sea flux from satellite data. In *Ocean Circulation and Climate*, ed. G. Siedler, J. Church, and J. Gould, 173-179. New York: Academic Press.
- Liu, W. T.**, H. Hu, and **S. Yueh**. 2000. Interplay between wind and rain observed in Hurricane Floyd. *Eos* 81:253, 257.
- Liu, W. T.**, X. Xie, P. S. Polito, S. Xie, and H. Hashizume. 2000. Atmosphere manifestation of tropical instability waves observed by QuikSCAT and Tropical Rain Measuring Missions. *Geophys. Res. Lett.* 27:2545-2548.
- Liu, Y., M. Y. Su, X. H. Yan, and **W. T. Liu**. 2000. The mean-square slope of ocean surface waves and its effects on radar backscatter. *J. Atmos Ocean. Tech.* 17:980-993.
- Lobell, D., G. Asner, B. Law, and **R. Treuhaft**. 2001. Sub-pixel canopy cover estimation of coniferous forest using SWIR imaging spectrometry. *J. Geophys. Res.* 106:5151-5160.
- MacPherson, B., S. A. Gonzalez, **X. Pi**, M. C. Kelley, G. J. Bailey, M. P. Sulzer, **G. A. Hajj**, M. J. Buonsanto, and C. Wang. 2000. Comparison between SUPIM simulations and measured TEC for the January 1997 storm. *Geophys. Res. Lett.* 27:2845-2848.
- Makela, J. J., S. A. Gonzalez, B. MacPherson, **X. Pi**, M. C. Kelley, and P. J. Sultan. 2000. Intercomparisons of total electron content measurements using the Arecibo incoherent scatter radar and GPS. *Geophys. Res. Lett.* 27:2841-2844.
- Makela, J. J., M. C. Kelley, J. J. Sojka, **X. Pi**, and A. J. Mannucci. 2001. GPS normalization and preliminary modeling results of total electron content during a midlatitude space weather event. *Radio Sci.* 36:351-361.
- Marcus, S. L.**, **J. O. Dickey**, and O. de Viron. 2001. Links between intraseasonal (extended MJO) and ENSO timescales: insights via geodetic and atmospheric analysis. *Geophys. Res. Lett.* 28:3465-3468.
- Martonchik, J.V., **R. A. Kahn**, D. J. Diner, and R. A. West. 2001. Comments on: retrieval of aerosol properties over the ocean using multispectral and multiangle photopolarimetric measurements from the research scanning polarimeter. *Geophys. Res. Lett.* 28:3275-3276.
- Ménard, Y., **L.-L. Fu**, P. Escudier, and G. Kunstmann. 2000. Cruising the ocean from space with Jason-1 in the 2000s. *Eos* 81:381, 390-391.

- Menemenlis, D.**, and M. Chechelnitsky. 2000. Error estimates for an ocean general circulation model from altimeter and acoustic tomography data. *Mon. Wea. Rev.* 128:763-778.
- Milliff, R. E., M. H. Freilich, **W. T. Liu**, R. Atlas, W. G. Large. 2001. Global ocean surface vector wind observations from space. In *Observing the Oceans in the 21st Century*, ed. C. J. Koblinsky and N. R. Smith, 102-119. Melbourne: Bureau of Meteorology.
- Mitchum, G. T., R. Cheney, **L.-L. Fu**, C. Le Provost, Y. Menard, and P. Woodworth. 2001. The future of sea surface height observations. In *Observing the Oceans in the 21st Century*, ed. C. J. Koblinsky and N. R. Smith, 120-136. Melbourne: Bureau of Meteorology.
- Nakamura, M., and **Y. Chao**. 2000. Characteristics of three-dimensional quasi-geostrophic transient eddy propagation in the vicinity of a simulated Gulf Stream. *J. Geophys. Res.* 105:11385-11406.
- Nakamura, M., and **Y. Chao**. 2000. On the eddy thickness diffusivity of the Gent-McWilliams subgrid mixing parameterization. *J. Climate* 13:502-510.
- Nakamura, M., and **Y. Chao**. 2001. Diagnoses of an eddy-resolving Atlantic Ocean model simulation in the vicinity of the Gulf Stream; I: Potential vorticity. *J. Phys. Oceanogr.* 31:353-378.
- Nghiem, S. V.**, **F. K. Li**, E. Walsh, and S.-H. Lou. 2000. Radar backscatter across the Gulf Stream sea surface temperature front. *IEEE Trans. Geosci. Remote Sens.* 38:926-941.
- Pan, J., X.-H. Yan, Q. Zheng, and **W. T. Liu**. 2001. Scatterometers observe the variation of the Walker Circulation. *Eos* 82:536-537.
- Pan, J., X.-H. Yan, Q. Zheng, and **W.T. Liu**. 2001. Vector empirical orthogonal modes of the ocean surface wind variability derived from satellite scatterometer data. *Geophys. Res. Lett.* 28:3951-3954.
- Perigaud, C.**, and C. Cassou. 2000. Importance of oceanic decadal trends and westerly wind bursts for forecasting El Niño. *Geophys. Res. Lett.* 27:389-392.
- Perigaud, C.**, C. Cassou, B. Dewitte, **L.-L.Fu**, and D. J. Neelin. 2000. Use of data to improve El Niño forecasts with intermediate coupled models. *Mon. Wea. Rev.* 128:3025-3049.
- Perigaud, C.**, F. Melin, and C. Cassou. 2000. ENSO simulated with intermediate coupled models and evaluated with observations over 1970-1996. Part I: importance of the off-equatorial variability. *J. Climate* 13:1605-1634.
- Pi, X.**, M. Mendillo, W. J. Hughes, M. J. Buonsanto, D. P. Sipler, J. Kelly, Q. H. Zhou, G. Lu, and T. J. Hughes. 2000. Dynamical effects of geomagnetic storms and substorms in the middle-latitude ionosphere: An observational campaign. *J. Geophys. Res.* 105:7403-7417.
- Pinty, B., M. M. Verstraete, N. Gobron, F. Roveda, Y. Govaerts, J. V. Martonchik, D. J. Diner, and **R. A. Kahn**. 2001. Exploitation of surface albedo derived from the Meteosat data to

characterize land surface changes. In *Remote Sensing and Climate Modeling: Synergies and Limitations*, ed. M. Beniston and M. M. Verstraete, 51-67. Dordrecht: Kluwer Academic Publishers.

Polito, P. S., O. T. Sato, and **W. T. Liu**. 2000. Characterization of the heat storage from TOPEX/Poseidon at four oceanographic sites. *J. Geophys. Res.* 105:16911-16921.

Polito, P. S., **W. T. Liu**, and W. Tang. 2000. Correlation-based interpolation of NSCAT wind data. *J. Atmos Ocean Tech.* 17:1016-1026.

Polito, P., J. P. Ryan, **W. T. Liu**, and F. P. Chavez. 2001. Oceanic and atmospheric anomalies of tropical instability waves. *Geophys. Res. Lett.* 28:2233-2236.

Price, S. F., R. A. Bindschadler, C. L. Hulbe, and **I. Joughin**. 2001. Post-stagnation behavior in the upstream regions of Ice Stream C, West Antarctica. *J. of Glacio.* 47:283-294.

Rignot, E. 2001. Rapid retreat and mass loss of Thwaites Glacier, West Antarctic. *J. Glaciol.* 47:213-222.

Rignot, E., G. Buscarlet, B. Csatho, S. Gogineni, W.B. Krabill, and M. Schmeltz. 2000. Mass balance of the northeast sector of the Greenland Ice Sheet: a remote sensing perspective. *J. Glaciol.* 46:265-273.

Rignot, E., K. Echelmeyer, and W. B. Krabill. 2001. Penetration depth of interferometric synthetic-aperture radar signals in snow and ice. *Geophys. Res. Lett.* 28:3501-3504.

Rignot, E., W. B. Krabill, S. P. Gogineni, and **I. Joughin**. 2001. Contribution to the glaciology of northern Greenland from satellite radar interferometry. *J. Geophys. Res.* 106:34007-34020.

Rignot, E., L. Padman, D. R. MacAyeal, and M. Schmeltz. 2000. Observations of ocean tides below the Filchner and Ronne Ice Shelves, Antarctica, using synthetic aperture radar interferometry: comparison with tide model predictions. *J. Geophys. Res.* 105:19615-19630.

Rosen, P. A., S. Hensley, **I. Joughin**, **F. K. Li**, S. Madsen, E. Rodriguez, and R. M. Goldstein. 2000. Synthetic aperture radar interferometry. *Proc. IEEE* 88:333-382.

Rothrock, D. A., **R. Kwok**, and D. Groves. 2000. Satellite views of the Arctic Ocean freshwater balance. In *The Freshwater Budget of the Arctic Ocean*, ed. E. Lyn Lewis, 409-452. Dordrecht, Kluwer Academic.

Sato, O. T., P. S. Polito, and **W. T. Liu**. 2000. Importance of salinity measurements in the heat storage estimation from TOPEX/Poseidon. *Geophys. Res. Lett.* 27:549-551.

Schmeltz, M., **E. Rignot**, and D. McAyeal. 2001. Ephemeral grounding as a signal of ice-shelf change. *J. Glaciol.*, 47:71-77.

- Siegert, M. J., and **R. Kwok**. 2000. Ice-sheet radar layering and the development of preferred crystal orientation fabrics between Lake Vostok and Ridge B, central East Antarctica. *Earth Planetary Sci. Lett.* 179:227-235.
- Siegert, M. J., **R. Kwok**, C. Mayer, and B. Hubbard. 2000. Water exchange between the subglacial Lake Vostok and the overlying ice sheet. *Nature* 403:643-646.
- Song, Y. T.**, and **Y. Chao**. 2000. An embedded bottom boundary layer formulation for z-coordinate ocean models. *J. Atmos. Oceanic Tech.* 17:546-560.
- Song, Y. T.**, D. B. Haidvogel, and S. M. Glenn. 2001. Effects of topographic variability on the formation of upwelling centers off New Jersey: a theoretical model. *J. Geophys. Res.* 106:9223-9240.
- Stammer, D., R. Bleck, C. Boening, P. De Mey, H. Hurlburt, **I. Fukumori**, C. Le Provost, R. Tokmakian, and M. Wentzel. 2001. Global ocean modelling and state estimation in support of climate research. In *Observing the Oceans in the 21st Century*, ed. C. J. Koblinsky and N. R. Smith, 511-528. Melbourne: Bureau of Meteorology.
- Studinger, M., R. E. Bell, D. D. Blankenship, C. A. Finn, R. A. Arko, D. L. Morse, and **I. Joughin**. 2001. Subglacial sediments: a regional geological template for ice flow in West Antarctica. *Geophys. Res. Lett.* 28:3493-3496.
- Talley, L. D., D. Stammer, and **I. Fukumori**. 2001. Towards a WOCE Synthesis. In *Ocean Circulation and Climate*, ed. G. Siedler, J. Church, and J. Gould, 525-545. San Diego: Academic Press.
- Thomas, A. C., J. L. Blanco, **M.-E. Carr**, P. T. Strub, and J. Osses. 2001. Variability of satellite-measured chlorophyll and temperature off northern Chile during the 1996-1998 La Niña and El Niño. *J. Geophys. Res.* 106:899-915.
- Thomas, R. H., W. Abdalati, T. Akins, B. Csatho, E. Frederick, P. Gogineni, W. Krabill, S. Manizade, and **E. Rignot**. 2000. Substantial thinning of a major east Greenland outlet glacier. *Geophys. Res. Lett.* 27:1291-1294.
- Tratt, D. M.**, R. J. Frouin, and D. L. Westphal. 2001. April 1998 Asian dust event: a southern California perspective. *J. Geophys. Res.* 106:18371-18379.
- Treuhart, R. N.**, and P. R. Siqueira. 2000. Vertical structure of vegetated land surfaces from interferometric and polarimetric radar. *Radio Sci.* 35:141-177.
- Treuhart, R. N.**, **S. T. Lowe**, **C. Zuffada**, and **Y. Chao**. 2001. 2-cm GPS altimetry over Crater Lake. *Geophys. Res. Lett.* 28:4343-4346.
- Vaughan, D. G., A. M. Smith, H. Corr, A. Jenkins, C. R. Bentley, M. D. Stenoien, S. S. Jacobs, T. B. Kellog, **E. Rignot**, and B. K. Lucchitta. 2000. A review of ice-sheet dynamics in the Pine Island Glacier basin, West Antarctica: hypothesis of instability versus observations of change. In

The West Antarctic Ice Sheet: Behavior and Environment, ed. R. Alley and R. Bindshadler, 237-256. Washington D.C.: American Geophysical Union.

Wang, L., **Y. Chao**, C. J. Koblinsky, and S. Howden. 2000. Influence of lateral boundaries on mesoscale variability. *Geophys. Res. Lett.* 27:709-712.

Weichman, P. B., and **R. E. Glazman**. 2000. Passive scalar transport by travelling wave fields. *J. Fluid Mech.* 420:147-200.

Weinstock, E. M., E. J. Hints, D. B. Kirk-Davidoff, J. G. Anderson, A. E. Andrews, **R. L. Herman**, C. R. Webster, M. Loewenstein, J. R. Podolske, and T. P. Bui. 2001. Constraints on the seasonal cycle of stratospheric water vapor using in situ measurements from the ER-2 and a CO photochemical clock. *J. Geophys. Res.* 106:22707-22724.

Wilson, W. J., **S. H. Yueh**, S. J. Dinardo, S. Chazanoff, A. Kitiyakara, **F. K. Li**, and Y. Rahmat-Samii. 2001. Passive Active L- and S-band (PALS) microwave sensor for ocean salinity and soil moisture measurements. *IEEE Trans. Geosci. Remote Sens.* 39:1039-1048.

Xie, S. P., **W. T. Liu**, Q. Liu, and M. Nonaka. 2001. Far-reaching effects of the Hawaiian Island on the Pacific ocean-atmosphere. *Science* 292:2057-2060.

Yu, J. Y., **W. T. Liu**, and C. R. Mechoso. 2000. The SST anomaly dipole in the northern subtropical Pacific and its relationship with ENSO. *Geophys. Res. Lett.* 27:1931-1934.

Yueh, S. H., B. Stiles, W.-Y. Tsai, H. Hu, and **W. T. Liu**. 2001. QuikSCAT geophysical model function for tropical cyclones and application to Hurricane Floyd. *IEEE Trans. Geosci. Remote Sensing* 39:2601-2612.

Yueh, S. H., R. West, **F. K. Li**, W.-Y. Tsai, and R. Lay. 2000. Dual-polarized Ku-band backscatter signatures of hurricane ocean winds. *IEEE Trans. Geosci. Remote Sens.* 38:73-88.

Yueh, S. H., R. West, W. J. Wilson, **F. K. Li**, E. G. Njoku, and Y. Rahmat-Samii. 2001. Error sources and feasibility for microwave remote sensing of ocean surface salinity. *IEEE Trans. Geosci. Remote Sens.* 39:1049-1060.

Zheng, Q., X.-H. Yan, **W. T. Liu**, V. Klemas, and D. Sun. 2001. Space Shuttle observations of open ocean oil slicks. *Remote Sens. Environ.* 76:49-56.

Appendix B.

Acronyms



Appendix B.

Acronyms

ARMAR	Airborne Rain Mapping Radar
CAMEX-4	Convection and Moisture Experiment - 4
CNES	Centre National d'Etudes Spatiales (French Space Agency)
C-ICE	Collaborative Interdisciplinary Cryospheric Experiments
ECCO	Estimating the Circulation and Climate of the Ocean
ECMWF	European Center for Medium Range Weather Forecast
ENVISAT	Environmental Satellite
ERS 1/2	European Remote-sensing Satellites 1 and 2
EUC	Equatorial Undercurrent
GCM	General Circulation Model
GFO	GEOSAT Follow-On
GIM	Global Ionospheric Maps
GLOBE	Global Backscatter Experiment
GRACE	Gravity Recovery And Climate Experiment
GSFC	Goddard Space Flight Center
IRI	International Reference Ionosphere
ITF	Indonesian Throughflow
KWAJEX	Kwajalein Experiment
LDR	Linear Depolarization Rate
MERIS	Medium Resolution Imaging Spectrometer
MOM3	Modular Ocean Model, Version 3
NASA	National Aeronautics and Space Administration
NCEP	National Center for Environmental Prediction
NUBF	Non-Uniform Beam-Filling
OAM	Oceanic Angular Momentum
PDO	Pacific Decadal Oscillation
PR	Precipitation Radar
RGPS	RADARSAT Geophysical Processor System
RMS	Root Mean Square
ROMS	Regional Ocean Modeling System
SAR	Synthetic Aperture Radar
SeaWiFS	Sea-viewing Wide Field-of-view Sensor
SHEBA	Surface Heat Budget of the Arctic Ocean
TAO	Tropical Atmosphere and Ocean
TEC	Total Electron Count
TECU	Total Electron Content Units
TEFLUN-B	Texas-Florida Underflights, Part B
TOMS	Total Ozone Mapping Spectrometer on Nimbus 7
TOPEX	Ocean Topography Experiment
TRMM	Tropical Rainfall Measuring Mission
UV	Ultraviolet
XBT	Expendable Bathythermograph



